

Russian-German Cooperation Laptev-Sea System



Expedition TRANSDRIFT XIII
April 5 - May 5, 2008

CONTENTS

ABBREVIATIONS AND ACRONYMS.....	5
INTRODUCTION	7
Timokhov, L., Kassens, H., Novikhin, A., Kirillov, S.	
METEOROLOGICAL MEASUREMENTS AT THE ICE EDGE OF THE WEST NEW SIBERIAN POLYNYA.....	11
Heinemann, G., Helbig, A., Ernsdorf, T.	
ICE THICKNESS MEASUREMENTS: HEM CAMPAIGN DATA REPORT	23
Krumpen, T., Rabenstein, L., Hendricks, S., Hoelemann, J.	
ICE PHYSICS INVESTIGATIONS	35
Tyshko, K.	
OCEANOGRAPHIC INVESTIGATIONS.....	41
Kirillov, S., Dmitrenko, I., Makhotin, M., Klagge, T., Hoelemann, J.	
FIRST USE OF A FREE-DRIFTING PROFILING FLOAT (NEMO) IN THE LAPTEV SEA POLYNYA	47
Klagge, T., Hoelemann, J.	
HYDROCHEMICAL OBSERVATIONS.....	51
Novikhin, A.	
BIOLOGICAL INVESTIGATIONS.....	55
Abramova, E., Gukov, A.	
PRELIMINARY SCIENTIFIC AND PRACTICAL RESULTS OF THE POLYNYA 2008/TRANSDRIFT XIII EXPEDITION.....	61
Timokhov, L., Kassens, H., Novikhin, A., Kirillov, S.	
REFERENCES	63
APPENDIX	65

ABBREVIATIONS AND ACRONYMS

AARI	State Research Center – Arctic and Antarctic Research Institute
ADCP	Acoustic Doppler Current Profiler
AWI	Alfred Wegener Institute for Polar and Marine Research
AWS	Automatic Weather Station
CTD	Conductivity Temperature Depth Meter
DOY	Day of the year
DWD	German Meteorological Service
EM Bird	Electromagnetic Bird
ENVISAT	Environmental Satellite of the European Space Agency
GME	Global Model of the German Meteorological Service
GPS	Global Positioning System
IFM-GEOMAR	Leibniz Institute of Marine Sciences
IPY	International Polar Year
OSL	Otto Schmidt Laboratory for Polar and Marine Research
SAR	Synthetic Aperture Radar
WNS	West New Siberian

INTRODUCTION

L. Timokhov¹, H. Kassens², A. Novikhin¹, S. Kirillov¹

¹State Research Center – Arctic and Antarctic Research Institute, St.Petersburg, Russia

²IFM-GEOMAR, Leibniz Institute of Marine Sciences, Kiel, Germany

1. Recent climate changes in the Arctic

The climate system of the Arctic is currently undergoing evident changes. Extreme strengthening of cyclonic activity and air temperature rise are responsible for considerable changes in the Arctic Ocean. During the last decade, an anomalous rise in the temperature of inflowing Atlantic waters was recorded, which in some regions exceeded the values ever observed during the 150 years of historical observations (ACIA, 2004; Polyakov et al., 2004, 2005). During the last 50 years both the extent and thickness of sea-ice cover have diminished (Johannessen et al., 1995; Maslanik et al., 1996; Rothrock et al., 1999; Haas, 2004). The reduction is still evident especially during the summer months. Also the timing of the main seasonal events has shifted. For instance, spring ice melting starts earlier while freeze-up in autumn is delayed.

The observed anomalies of major climate-driving processes (atmospheric, ice and oceanic) together with anomalous weather conditions demand a reliable and correct evaluation of the modern situation and forecast of future Arctic development. It is necessary to track similar changes back in time for the whole period of observations and to understand the possible forcing and feedback mechanisms.

The natural system of the Siberian Arctic shelves is especially sensitive to climate changes. Climate models and paleoclimatic reconstructions reveal that variations in the size of continental ice sheets and ice caps as well as sea ice cover extent affect the global ocean circulation. The Siberian hinterland adjacent to the Laptev Sea is the dominant source of freshwater for the Arctic Ocean, thus predetermining intensive sea ice production on the Laptev Sea shelf, which is an important component of the global climate system.

Modern climate scenarios predict a considerable rise of the average annual air temperature in the Arctic by 3-5°C on land and 7°C over the sea, especially during the winter season. An increase in precipitation and river runoff (by 25%) is expected for winter and spring. The anticipated sea-level rise in the Arctic might reach 90 cm. The environmental changes of the Siberian shelves caused by these climate changes will affect the social and economic life in the region. Therefore, investigation of the climatically sensitive Arctic environment can give an early warning about the onset of changes which might also affect regions outside the polar realm.

The Arctic seas form a transitional zone between the arctic coastal regions and the deep-sea basins. Climate-driving mechanisms, such as atmospheric circulation, sea-ice cover and river runoff, are especially variable in the Arctic marginal seas (Dmitrenko et al., 2007; Kirillov et al., in press). The Arctic atmospheric circulation characterized by cyclones and anticyclones initiates the system of currents and affects the spreading of riverine water on the shelf during summer (Dmitrenko et al., 2005a), which in turn determines the position of ocean fronts. Climate-driven variability in sea ice extent, hydrological and hydrochemical regimes, biological activity, sedimentation and environmental conditions depends on the respective season.

The strong seasonality of the Arctic seas is essential for the processes of front formation both in the ocean and in the atmosphere. The seasonal variability of the arctic sea ice cover extent results in evident albedo fluctuations. During summer there are temperature and salinity

contrasts between the southern regions influenced by relatively warm freshwater inflow and the northern regions covered by melting pack ice. The system of fronts is represented by narrow zones with sharp lateral and vertical gradients in hydrological and hydrochemical characteristics as, for instance, an interface between fresh riverine and saline seawater.

The system of flow leads (polynyas) is an essential component of the Arctic marine environment. Polynyas are open-water areas formed in winter between the fast and drift ice. Sometimes they are covered by newly formed ice. Due to the constantly blowing southerly winds polynyas can be up to 100 km wide. Polynyas induce thermodynamic anomalies of the surface water layer. The combination of extremely low air and water temperatures and high current velocities in polynya regions favour sea ice formation and, thus, a local increase in salinity (Dmitrenko et al., 2005b). Previous investigations have shown that the Laptev Sea polynya system is extremely sensitive to changes in atmospheric circulation. At the same time, the evaluations show that an intensive energy exchange between water surface and atmosphere in polynyas during winter influences the atmospheric circulation. Frontal zones and polynya systems are good indicators of climate-driven variability in marine systems. The Laptev Sea is a key region for investigations aimed at understanding the driving mechanisms and evaluating the response of Arctic environment to global climate change as it includes such important natural components as:

- a long frontier with the deep ocean,
- a terrestrial hinterland with a dynamic coastal zone,
- a huge amount of freshwater input,
- submarine and terrestrial permafrost,
- a seasonally changeable ice cover,
- a vast polynya system.

At the 11th Workshop within the Framework of Cooperation in Marine and Polar Research between the Russian Ministry for Education and Science and the German Federal Ministry for Education and Research (October 23-25, 2006, Schleswig) the Russian-German project “The Eurasian Shelf Seas in the Arctic’s Changing Environment: Frontal zones and polynya systems in the Laptev Sea” was signed. The project is part of the “Laptev Sea System” research program. It is aimed at evaluating climatically induced changes in the Laptev Sea region through the study of frontal zones and polynya systems (Fig. 1).

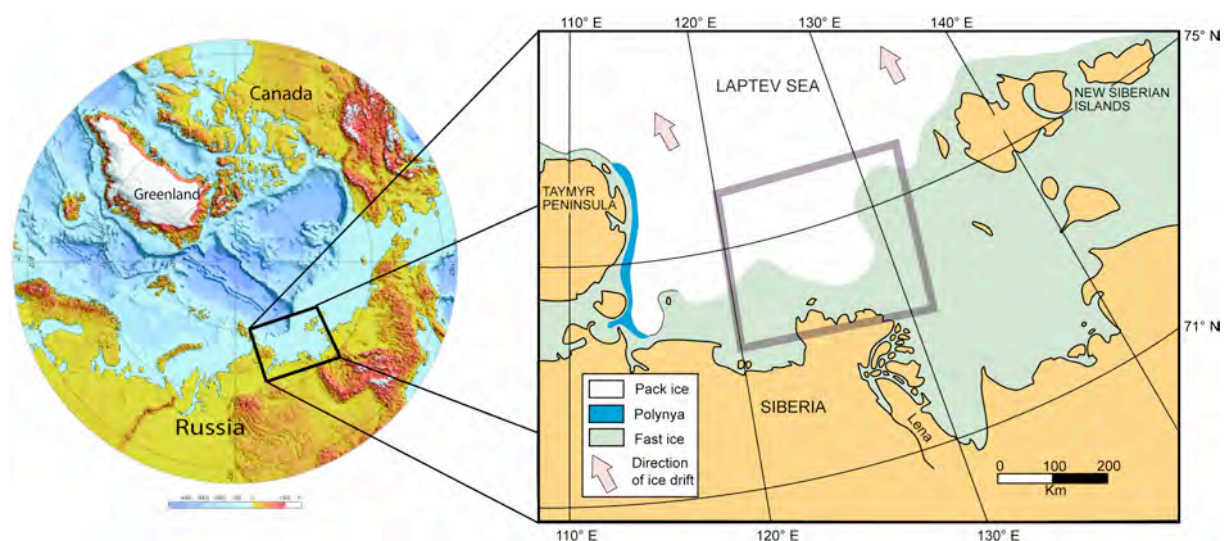


Fig. 1: Working area of the project Laptev Sea System.

2. Expedition goals and tasks

The main goal of the POLYNYA 2008/TRANSDRIFT XIII expedition is to investigate polynya systems and frontal zones in the Laptev Sea as indicators of climatically driven environmental changes in the Siberian shelf seas. The main research tasks are as follows:

- to investigate oceanographic, meteorological, hydrochemical and biological conditions together with bottom sediments in the southern part of the sea where the polynya and the frontal zone between riverine and seawater are located in winter;
- to investigate the processes responsible for formation, evolution and disappearance of the polynya system as the frontal zone between the fast and drift ice;
- to investigate thermohaline, hydrochemical and meteorological processes in polynyas and adjacent fast and drift ice regions;
- to determine lateral and vertical heat and salt fluxes induced by density stratification and bottom topography;
- to determine various states of polynyas and frontal systems dependent upon climate conditions in the Laptev Sea region;
- to evaluate the influence of environmental changes on the Arctic ecosystems and economic activity in the region;
- to gather evidence about the interannual cyclic variability of different parameters of marine systems in order to improve climate forecast models.

The tasks correspond to the main research initiatives of the IPY (International Polar Year) and the “Laptev Sea System” program. These are:

- to carry out oceanographic measurements at episodic stations;
- to perform water and ice sampling at oceanographic stations for chemical analysis and determination of the concentration and composition of suspended particulate matter;
- to collect biological samples at oceanographic stations;
- to carry out standard ice and meteorological observations;
- to perform a series of CTD (Conductivity Temperature Depth Meter) and ADCP (Acoustic Doppler Current Profiler; current velocity and direction) measurements;
- to measure ice thickness along transects from the coast to the drift ice with a helicopter-borne EM-Bird (electro-magnetic induction sounding).

METEOROLOGICAL MEASUREMENTS AT THE ICE EDGE OF THE WEST NEW SIBERIAN POLYNIA

G. Heinemann, A. Helbig, T. Ernsdorf

Trier University, Trier, Germany

1. Introduction

During the expedition TRANSDRIFT XIII-2 the meteorological regime was studied at four different sites along the ice edge of the West New Siberian Polynya during the period from April 11 to 29, 2008 in high temporal resolution using Automatic Weather Stations (AWS). The data were post-processed (including calibration and validation) and are available as 10min and 1h averages.

This data report provides information on the properties of the meteorological sensors and the locations of the AWS and presents a comparison of measurements at the four sites. It also provides an overview of the general meteorological situation of the field experiment using synoptic analysis maps.

2. Description of AWS

2.1. Meteorological sensors

To ensure that data loss was minimized, parallel measurements of air temperature and horizontal wind vector were carried out with different sensors on the AWS. The properties of the sensors are described below.

2.1.1. Wind speed and wind direction

Ultrasonic Anemometer UsA 2D

Range:	0-60 m/s, accuracy $\pm 2\%$
Resolution:	0.01 m/s
Data rate:	1-4 Hz
Output:	Wind direction and wind speed or u- and v-components

Young Wind Monitor Model 05103

Range:	0-100 m/s
Resolution:	Speed ± 0.3 m/s, 1% Direction $\pm 3^\circ$
Starting speed:	1 m/s
Signal:	magnetically induced AC voltage, 3 pulses per revolution Azimuth potentiometer

2.1.2. Air temperature and humidity

Campbell Scientific CS215

Accuracy:	
Rel. humidity:	$\pm 4\%$
Air temperature	$\pm 0.9^\circ\text{C}$ (-40°C to $+70^\circ\text{C}$)

The relative humidity sensor indicated refers to a saturation above water surface. The data set records contain the specific humidity (g/kg) instead of relative humidity.

Electric ventilated thermometer (Typ Frankenberger)

Platinum-Resistance Pt-100 according with DIN, tolerance ± 0.1 K at 0°C

2.1.3. Net radiation

NR_LITE Net Radiometer

Thermopile (upper and lower sensors provide the differential temperature)

Spectral range: 0.2-100 μm

Directional Error

($0-60^{\circ}$ at 1000 W/m^2): $< 30 \text{ W/m}^2$

Working temperature: -30°C to $+70^{\circ}\text{C}$

The cooling of the thermopiles by the wind (wind speed U) decreases the temperature difference between top and bottom used as the measure of the radiation balance Q_0 . Therefore Q_0 must be corrected using an empirical relationship specified by the manufacturer:

$Q_0, \text{cor} = Q_0, \text{obs}$ $U \leq 5 \text{ m/s}$

$Q_0, \text{cor} = Q_0, \text{obs} * (1.0 + 0.021286 * (U - 5.0))$ $U > 5 \text{ m/s}$

2.1.4. Barometric pressure

Barometric Pressure Sensor RPT410F

The barometric pressure readings in hPa were provided in relation to actual sensor height.

2.2. Height of sensors above ground

The tripods of the AWS were positioned directly on the flat and smooth fast ice, and were vertically adjusted and fastened with ice anchors. The sensors were mounted on each AWS at the same height above ground (fast ice). The snow cover on the fast ice varied between the four locations. The change of snow depth during the measurement period was negligible.

The sensor heights were as follows:

Air temperature, humidity		2.0 m above snow
Net radiation		1.6 m above snow
Wind speed, wind direction	Young	3.0 m above snow
	UsA 2D	2.8 m above snow

2.3. Data storage and transfer

For data storage a Data Logger Campbell CR1000 in conjunction with a memory card was used. The stored values are averages over 10 minutes. A transmission unit in connection with an omnidirectional antenna allowed the hourly data transfer via the ARGOS satellite to Trier University in order to monitor the data quality and sensor failures.

3. Sites of AWS

At all four sites identical AWS were deployed. The positions of the ice camps as well as the AWS are shown in Figure 2.

3.1. Ice camp 1 / TI0802

AWS ID: BLAU / AWS 1

Start of observation: 11.04.2008 17:15 YAT

End of observation: 05.05.2008 12:00 YAT

Coordinates: $73^{\circ} 48.293' \text{ N}$, $128^{\circ} 09.660' \text{ E}$

Situation:

Fast ice, thickness 65 cm, snow cover ca. 10 cm, 100 m south of the polynya ice edge, 100 m west of red tent (mooring station). Free air flow from all directions.

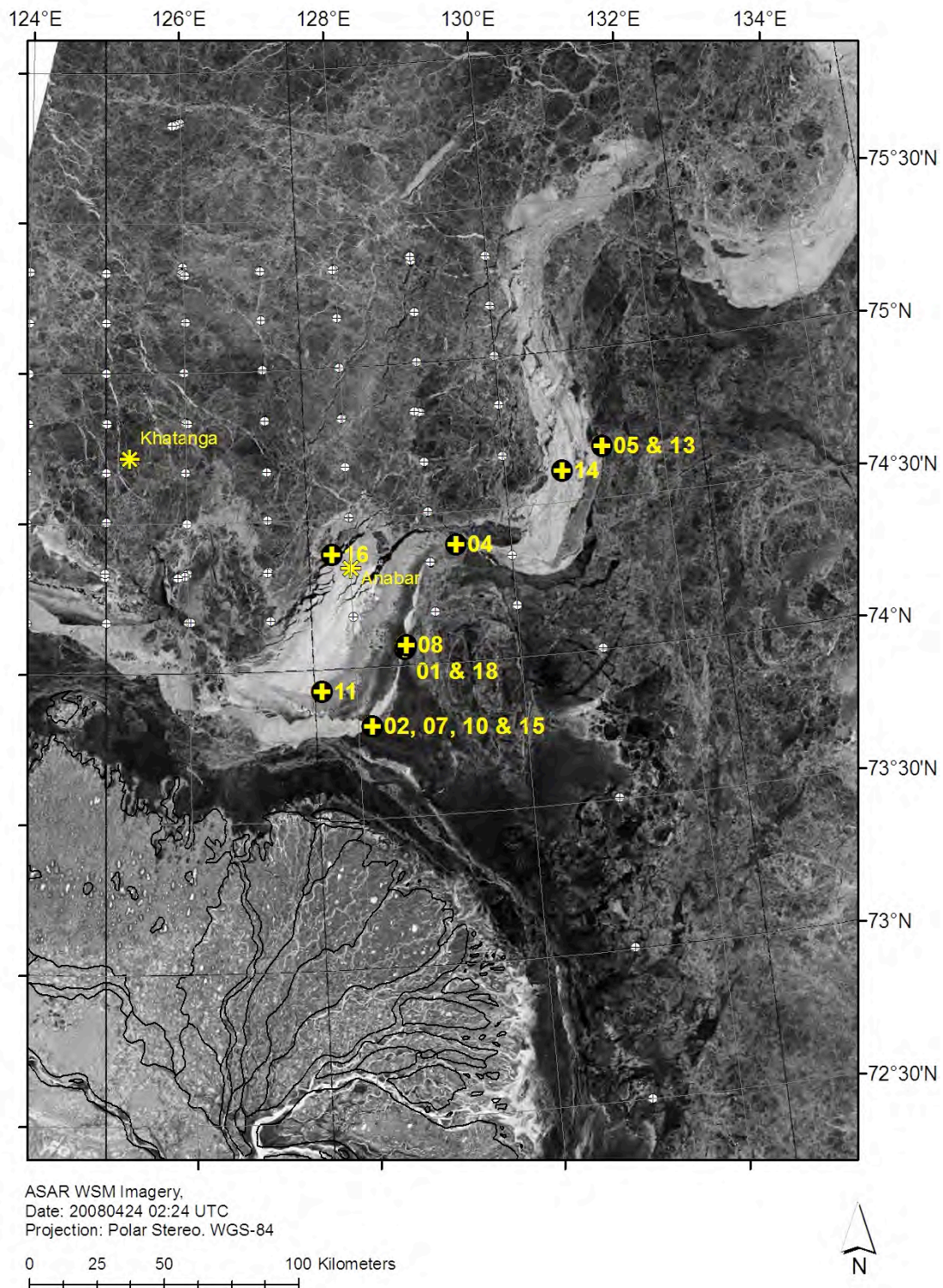


Fig. 2: Ice coverage and position of the West New Siberian-Polynya on April 24, 2008 as well as the positions of stations. The AWS are located at the stations 02 (AWS 1), 08 (AWS 4), 04 (AWS 2) and 05 (AWS 3).

3.2. Ice camp 2 / TI0804

AWS ID: ROT / AWS 2
Start of observation: 12.04.2008 14:15 YAT
End of observation: 29.04.2008 14:35 YAT
Coordinates: 74° 23.390' N, 129° 19.298' E
Situation: Fast ice, thickness 130 cm, snow cover ca. 10 cm, 400 m southeast of the Polynya ice edge, 200 m south of broken thinner ice, 100 m east of the mooring station. Free air flow from east and south.

3.3. Ice camp 3 / TI0805

AWS ID: GELB / AWS 3
Start of observation: 14.04.2008 16:00 YAT
End of observation: 29.04.2008 12:00 YAT
Ventilation: unplugged
Coordinates: 74° 40.368' N, 131° 14.752' E
Situation: Fast ice, thickness 106 cm, snow cover ca. 10 cm, in the neighborhood there were sastrugis up to 40 cm. 80 m east of broken pack ice with 0.8 m height, 200 m south of broken pack ice with a height of 0.6 m, 200 m northeast of the mooring station. Free air flow from east and south.

3.4. Ice camp 4 / TI0808

AWS ID: GRUEN / AWS 4
Start of observation: 24.04.2008 16:00 YAT
End of observation: 28.04.2008 13:30 YAT
Ventilation: unplugged
Coordinates: 74° 03.278' N, 128° 36.602' E
Situation: Fast ice, thickness 80 cm, snow cover ca. 8 cm, west of AWS pack-ice ridges up to heights of 1.8 m, new sea ice west in a distance of 200 m. Free air flow within a radius of 100 m.

4. Data structure

4.1. Description of the data set

The periods of the available data from the AWS at the different sites are shown in Table 1.

Table 1: Available data sets from the AWS.

AWS		April 2008																												
No.	Colour ID	11	12	13	14	15	16	17	18	19	20	21	22	23	24	25	26	27	28	29	30									
1	Blau																													
2	Rot																													
3	Gelb																													
4	Gruen																													

The observations by the AWS are provided in two files each (ASCII Format). In the file name, <colour> means the respective colour ID (see Table 1).

The files named 'CR1000_MW_10_<colour>_kal_1h.dat' contain all corrected and supplemented hourly mean values of the concerning AWS in chronological order (day of the

year (DOY), time in UTC).

The files named ‘CR1000_MW_10_<colour>_kal_f.dat’ contain additional quality flags for all observations. The contents of the files are described in detail in the file „readme.txt“.

4.2. Overview over the AWS data

Figure 3 gives an overview over wind direction, wind speed, net radiation, air pressure, air temperature and specific humidity at each AWS for the period April 11 to 29, 2008. Figure 4 shows a period of three days with a mesoscale high pressure system (see section 5).

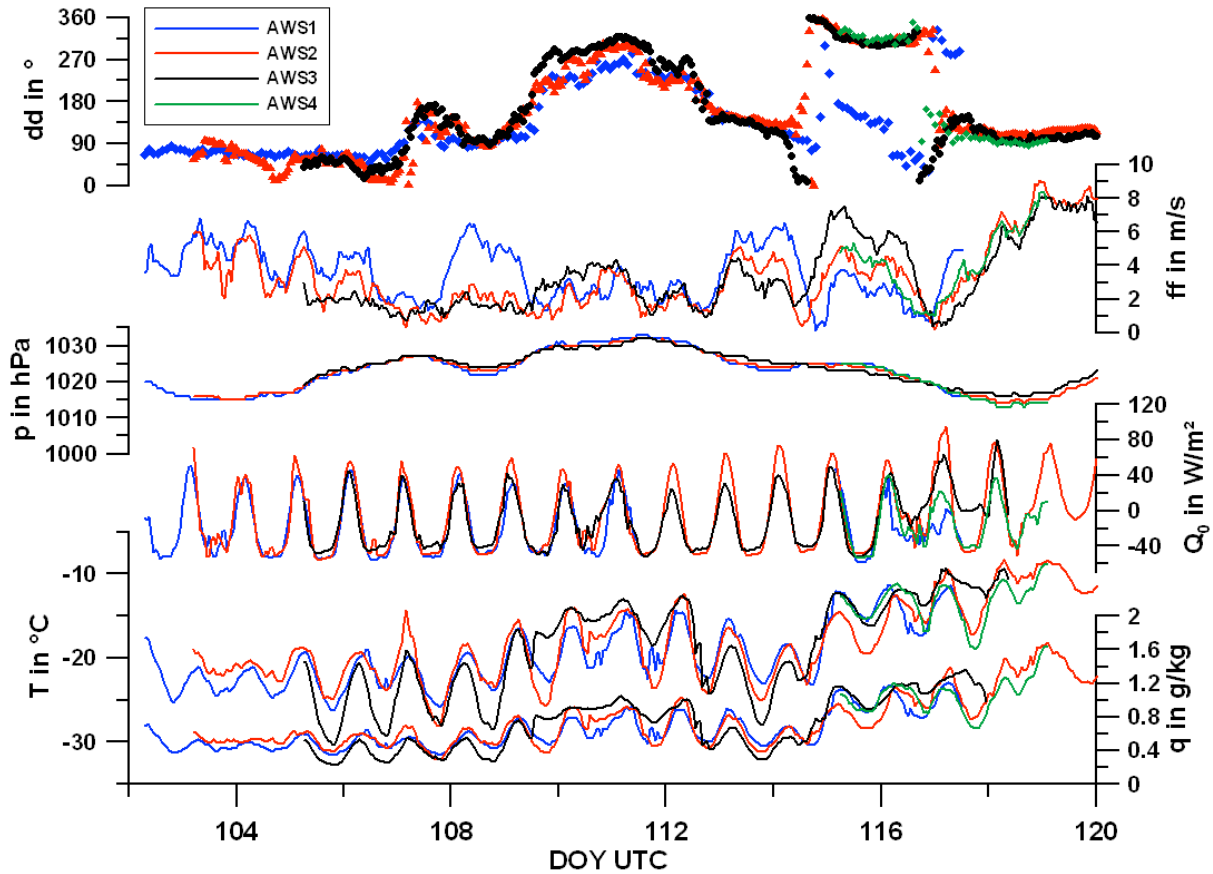


Fig. 3: Wind direction (dd), wind speed (ff), net radiation (Q_0), air temperature (T), air pressure and specific humidity (q) for the period April 11 (DOY 102) to April 29, 2008 (DOY 120) based on 1h averages.

5. General meteorological information

5.1. General synoptic situation

The synoptic situation was characterized by the influence of an anticyclone located in the Central Arctic with low cloudiness at middle and high levels, and weak winds with prevailing directions from E and SE. Minimum air temperatures in Tiksi were between -32°C (April 14 and 17) and -13°C (April 25). At the AWS on the sea ice, minimum air temperatures were down to -30°C and -20°C at the start and end of the field phase, respectively (Fig. 3).

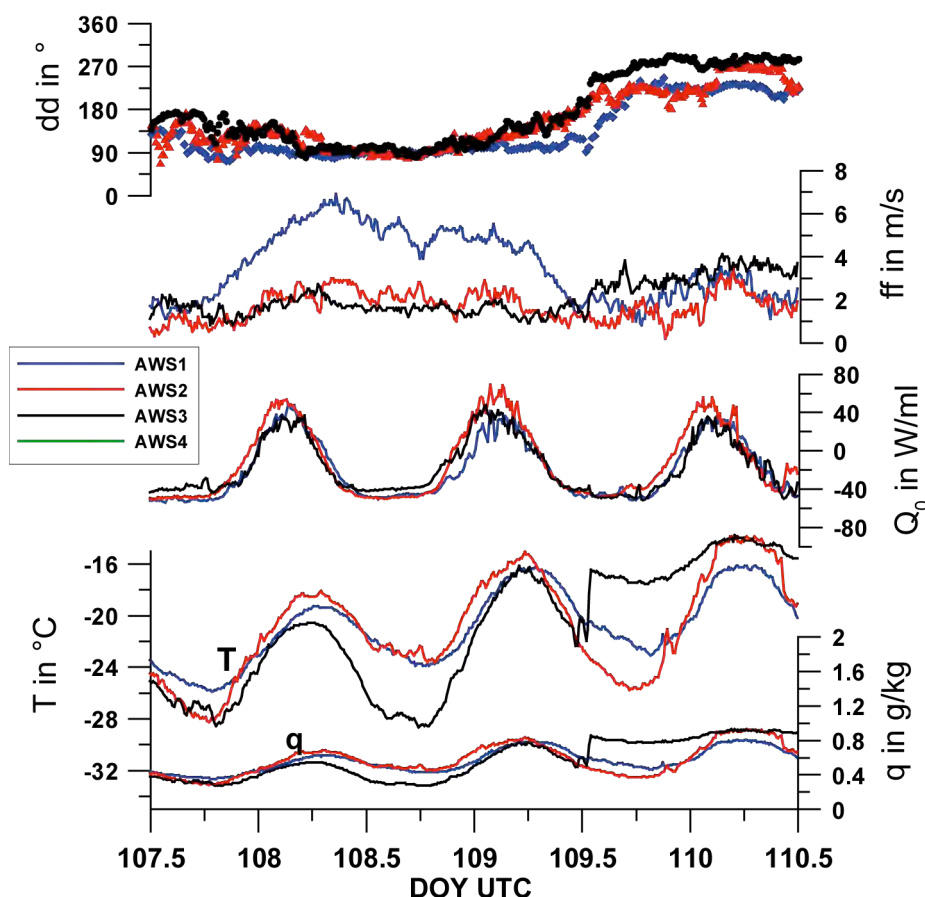


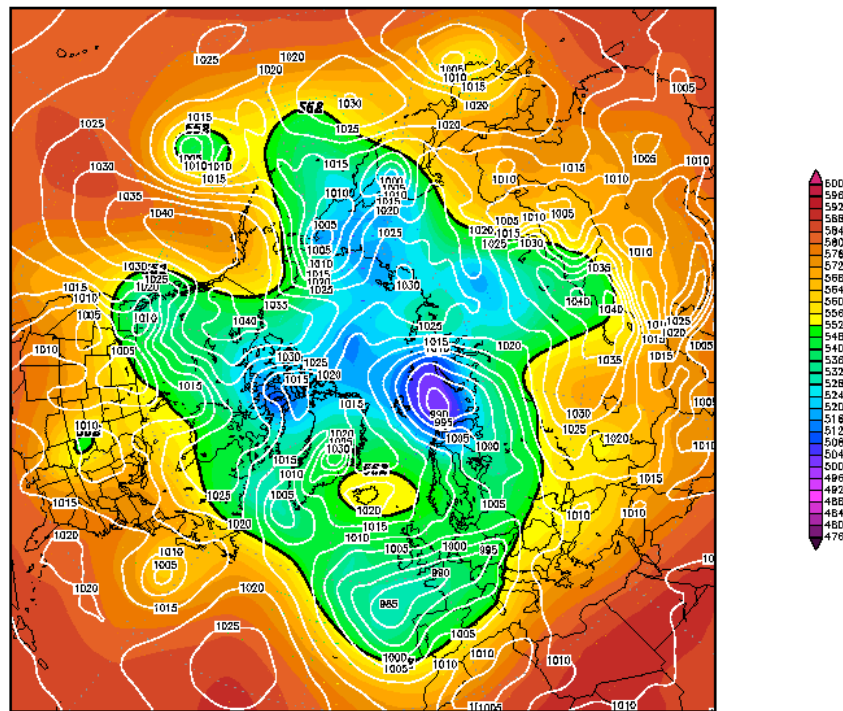
Fig. 4: Wind direction (dd), wind speed (ff), net radiation (Q_0), air temperature (T) and specific humidity (q) for the period April 16 (DOY 107) to April 19, 2008 (DOY 110) based on 10min averages.

The radiosonde ascents at 00 UTC at Tiksi (WMO Code 21824) have been collected and are available in the data base. Almost all temperature profiles show the surface inversion typical for persistent anticyclonic weather.

After weakening of the anticyclonic influence between April 18 (DOY 109) and April 22 (DOY 113) the region of Tiksi came under increasing influence of two low pressure systems: the first one located in the western part of the Kara Sea and the second one west of the Bering Street (Fig. 5). Low wind speeds correspond to small sea level pressure gradients. The wind directions varied between S and NNE. From April 25 to 27 light snowfall with moderate wind forces from E was observed while no precipitation occurred prior to April 25. In the period from April 28 to 30 low cloud cover dominated with winds from ESE and speeds of 5-7 m/s. The visibility achieved 2-3 km, but in the case of light snowfall it was lower. The working area of the expedition (250 km north of Tiksi) was very often under stronger anticyclonic impact with lower cloudiness than the region of Tiksi.

Valid: Sat,19APR2008 00Z

500 hPa Geopot. (gpdm) und Bodendruck (hPa)

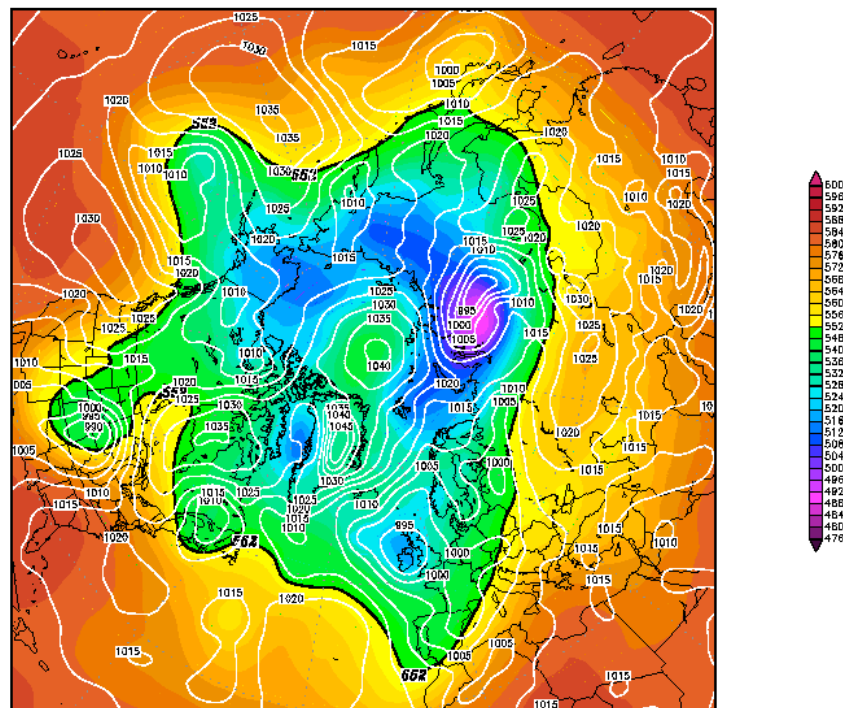


Daten: GFS-Modell des amerikanischen Wetterdienstes
(C) Wetterzentrale
www.wetterzentrale.de

Init : Fri,11APR2008 00Z

Valid: Fri, 11 APR 2008 00Z

500 hPa Geopot. (gpm) und Bodendruck (hPa)



Daten: GFS-Modell des amerikanischen Wetterdienstes
(C) Wetterzentrale
www.wetterzentrale.de

Fig. 5: Sea level pressure and geopotential at 500 hPa for April 11, 19 and 27, 2008 (from www.wetterzentrale.de).

Init : Sun,27APR2008 00Z Valid: Sun,27APR2008 00Z
 500 hPa Geopot. (gpm) und Bodendruck (hPa)

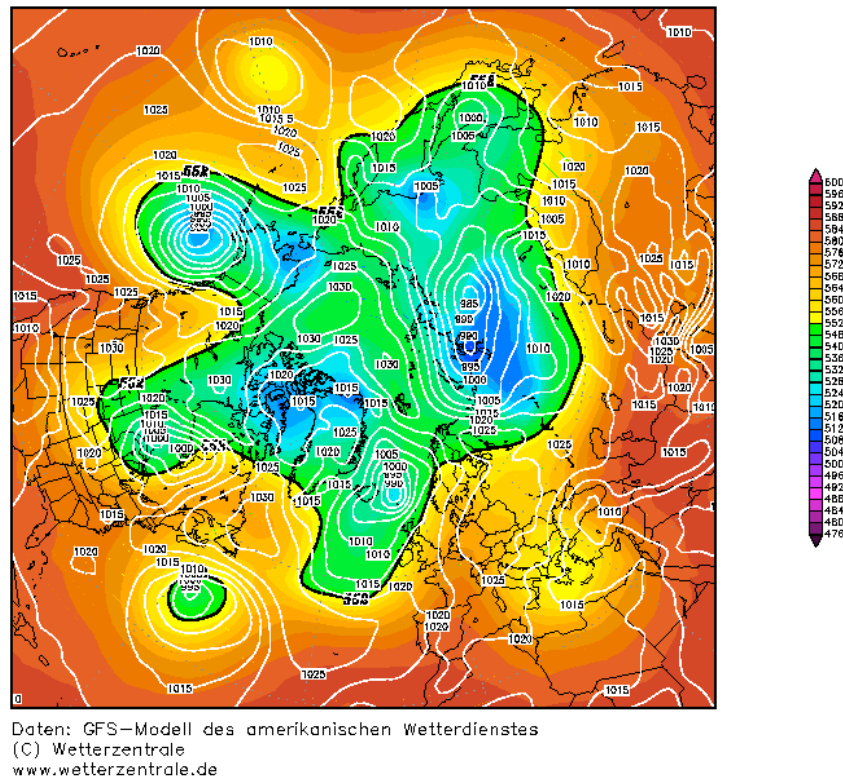
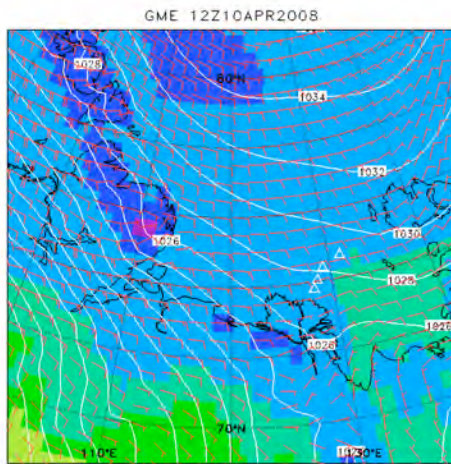


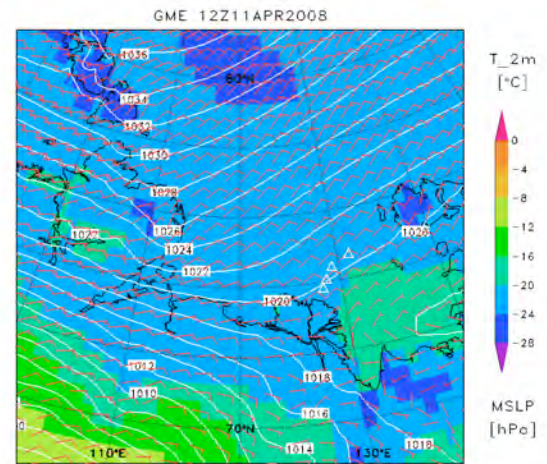
Fig. 5 (continued): Sea level pressure and geopotential at 500 hPa for April 11, 19 and 27, 2008 (from www.wetterzentrale.de).

5.2. Surface weather maps

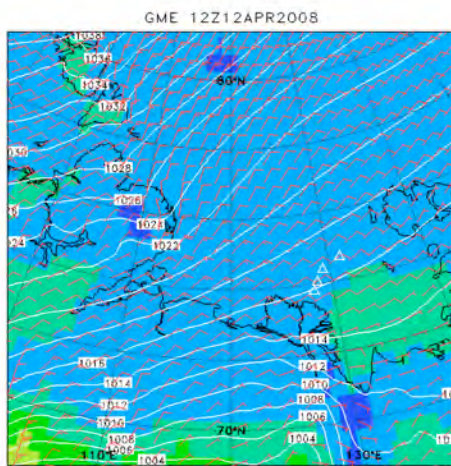
In order to document the synoptic situation day by day, the global GME (Global Model) analyses of the German Meteorological Service (DWD) for 12 UTC are shown for the period from April 10 to 30, 2008. The GME data are in the project database and are plotted for the subarea of the Laptev Sea. Figure 6 shows air temperature ($^{\circ}\text{C}$) at 2 m height above ground, air pressure (hPa) at mean sea level and horizontal wind vector at 10 m height above ground. The locations of the AWS are denoted by triangles. The pressure and wind fields on April 18, 2008 show a mesoscale anticyclone in the region of the AWS, which explains the large differences between the individual AWS in Figure 4. The observed different wind directions at different AWS locations on April 25, 2008 (see Fig. 3, DOY 116) also correspond clearly to the pressure pattern in the GME map.



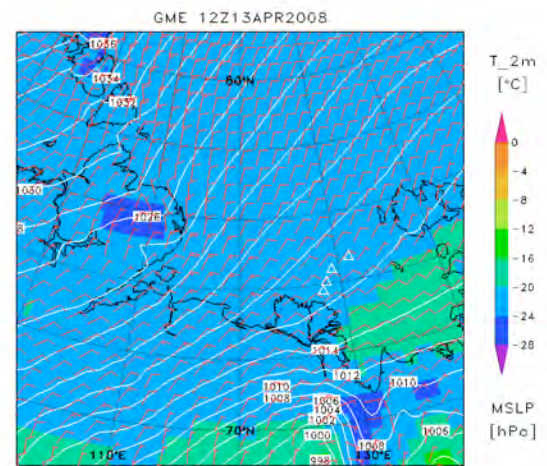
10. 04.2008



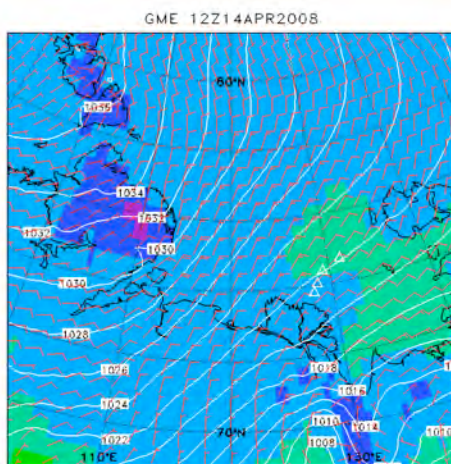
11.04.2008



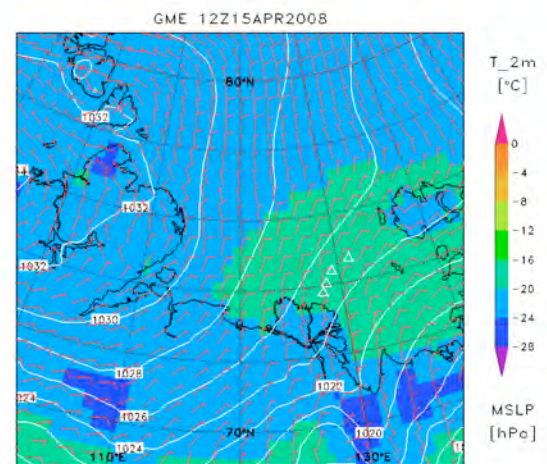
12.04.2008



13.04.2008

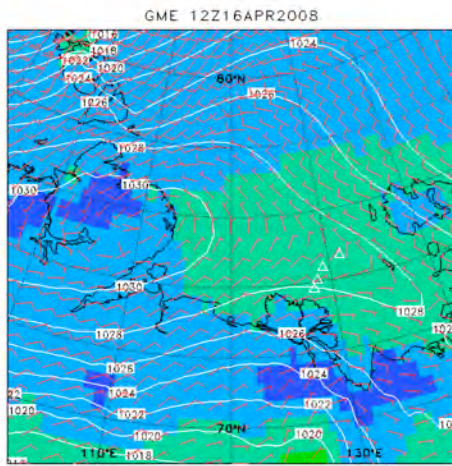


14.04.2008

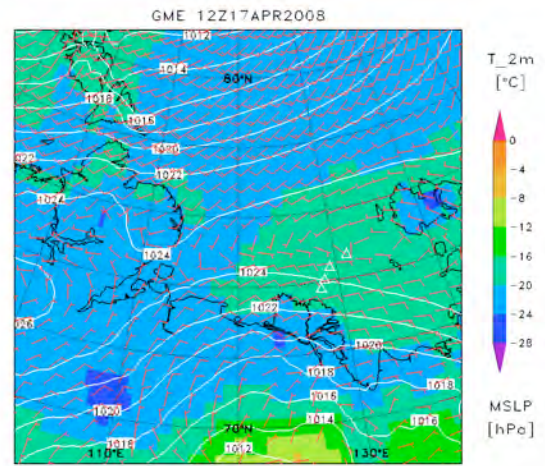


15.04.2008

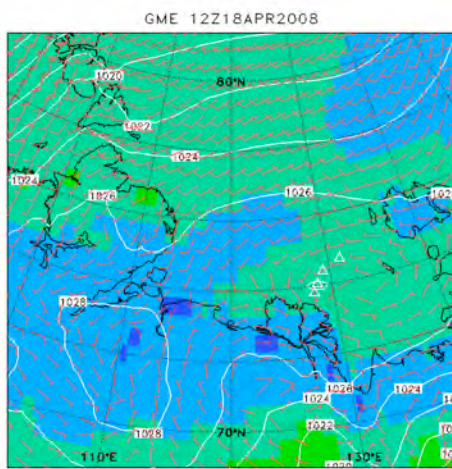
Fig. 6: Daily maps for air temperature (°C) at 2 m height above ground, air pressure (hPa) at mean sea level and horizontal wind vector at 10 m height above ground. The locations of the AWS are denoted by triangles.



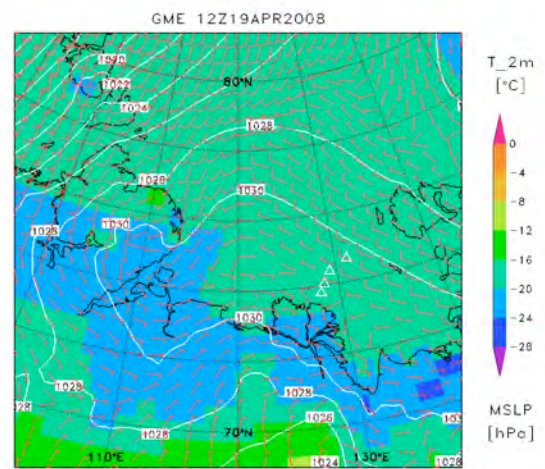
16.04.2008



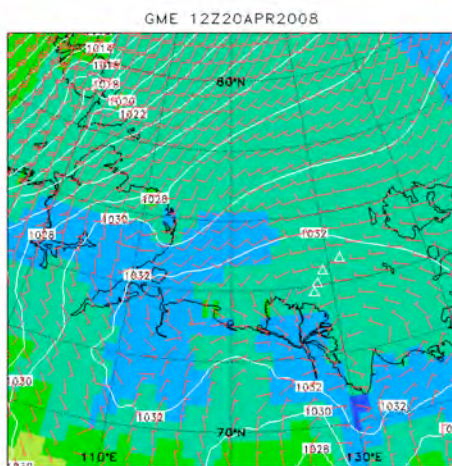
17.04.2008



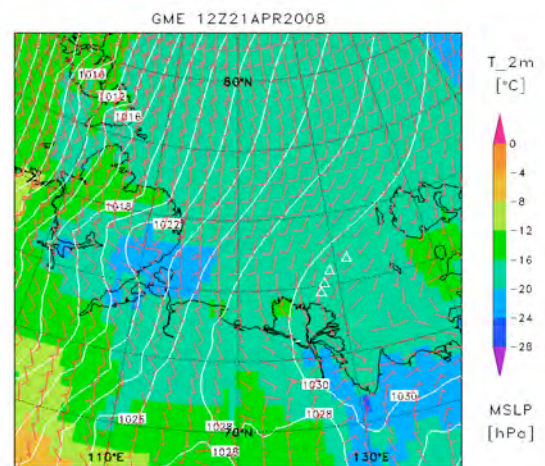
18.04.2008



19.04.2008

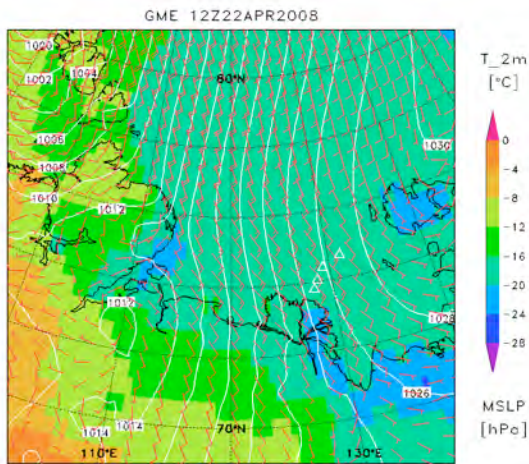


20.04.2008

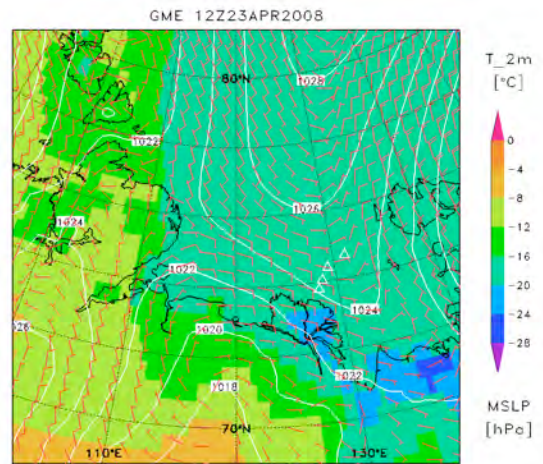


21.04.2008

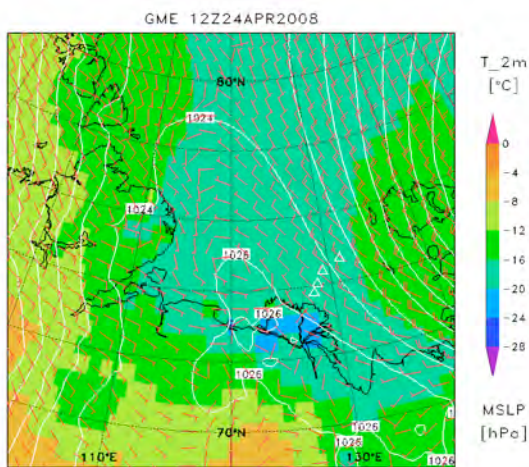
Fig. 6 (continued): Daily maps for air temperature (°C) at 2 m height above ground, air pressure (hPa) at mean sea level and horizontal wind vector at 10 m height above ground. The locations of the AWS are denoted by triangles.



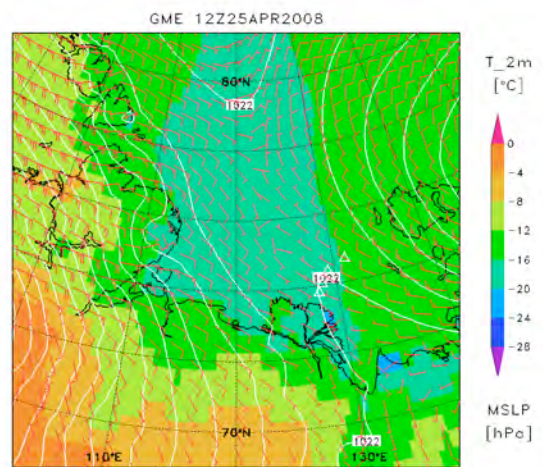
22.04.2008



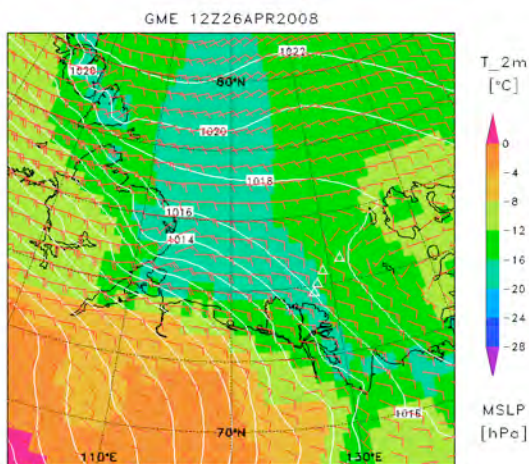
23.04.2008



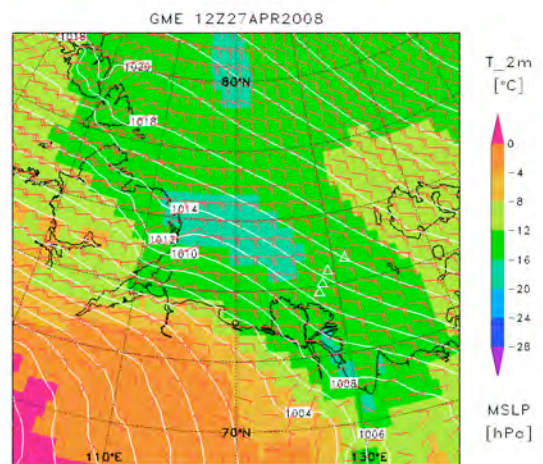
24.04.2008



25.04.2008

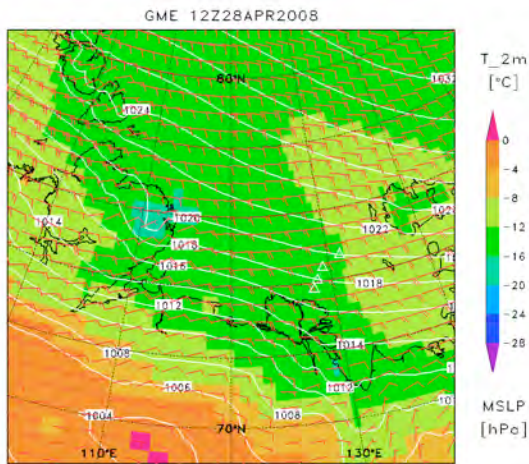


26.04.2008

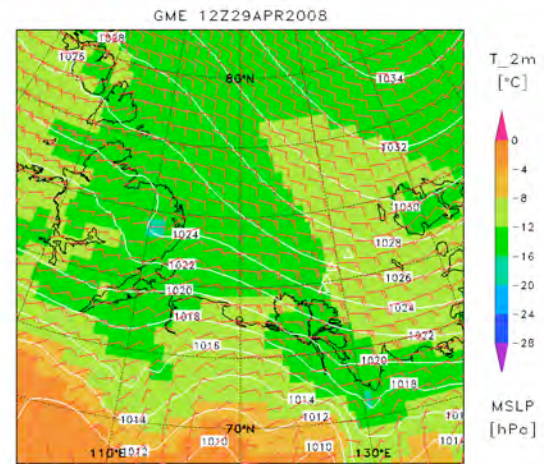


27.04.2008

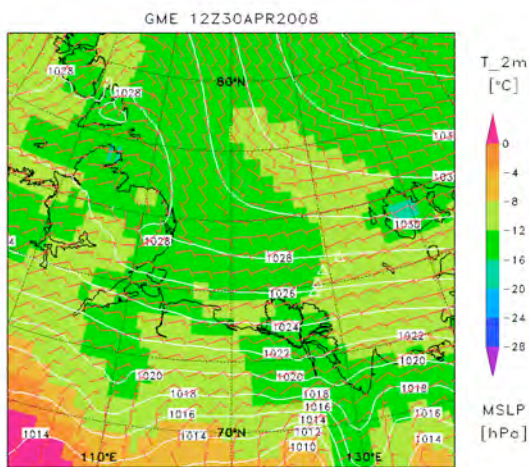
Fig. 6 (continued): Daily maps for air temperature (°C) at 2 m height above ground, air pressure (hPa) at mean sea level and horizontal wind vector at 10 m height above ground. The locations of the AWS are denoted by triangles.



28.04.2008



29.04.2008



30.04.2008

Fig. 6 (continued): Daily maps for air temperature (°C) at 2 m height above ground, air pressure (hPa) at mean sea level and horizontal wind vector at 10 m height above ground. The locations of the AWS are denoted by triangles.

ICE THICKNESS MEASUREMENTS: HEM CAMPAIGN DATA REPORT

T. Krumpen, L. Rabenstein, S. Hendricks, J. Hoelemann

Alfred Wegener Institute for Polar and Marine Research, Bremerhaven, Germany

1. Introduction

In recognition of its barely explored state, the ice thickness distribution along and across the West New Siberian (WNS) polynya was subject of the POLYNYA 2008/TRANSDRIFT XIII field campaign. To investigate the dynamics of polynya ice thickness and subsequent fluxes on a small-scale basis, helicopter-borne electromagnetic (EM) Bird flights were performed. Ice thickness profiles will be used to calibrate/validate a two-dimensional time-dependent steady-state flux model based on Morales Maqueda and Willmott (2000).

Here we present all tracks/profiles taken during the POLYNYA 2008/TRANSDRIFT XIII expedition.

2. Flight operation

All EM Bird flights across and along the WNS polynya were performed between April 10 and May 5, operated by Lasse Rabenstein and Thomas Krumpen.

After warming up the instrument (approx. 30 min), tracks were taken from the fast ice edge towards a pre-defined point of return and back. Start and end node, the point of return and track length were chosen according to a) the operating area of other work packages, b) available fuel capacity, c) weather conditions, and d) ice conditions. In total, 8 profiles were taken between April 10 and May 5, 2008. The flight time amounts to roughly 16 hours.

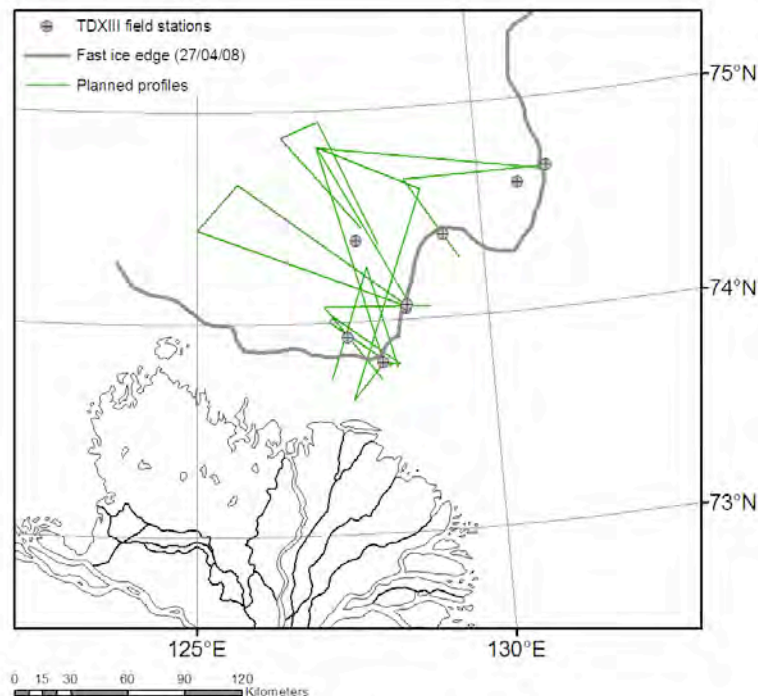


Fig. 7: EM BIRD flights planned between April 10 and May 5, 2008.

3. Activities

All planned activities related to the EM Bird sea ice thickness profiling are highlighted in Figure 7. Tracks were taken from the fast ice edge towards a pre-defined point of return and back. Simultaneously, a photogrammetric sea-ice survey was carried out.

3.1. EM tracks

The flight tracks contain 8 SE-NW transects, 3 E-W transects and one S-N transect, covering the WNS polynya from 73.6° N to 74°8' N and from 125.5° E to 131° E. Flight tracks are divided into profiles with a length of 20 minutes to half an hour to conduct in-flight instrument drift correction. The individual profiles are presented in the section “List of profiles”. Table 2 lists all tracks taken between April 10 and May 5, 2008.

Table 2: EM BIRD: List of all tracks

Profile ID	Comment
20080410	Test of instrument connectivity
20080414	Temporary instrument failures, coverage 60 %
20080416	Temporary instrument failures, coverage 40 %
20080419	Failure due to unstable power supply
20080424	No failure, complete coverage
20080428	No failure, complete coverage, second day of polynya opening
20080429	No failure, complete coverage, third day of polynya opening
20060505	No failure, complete coverage, 35% open water

3.2. Photogrammetric survey

During all flights, nadir-looking sea-ice photographs were taken. The average spatial coverage is 60 x 40 m. The temporal coverage is approximately 4 sec. Images will be used to aid Bird profile and ENVISAT-SAR image interpretation.

4. Processing

4.1. Basic principle

The EM system consists of a transmitter/receiver system for harmonic electromagnetic signals. The transmitter coil emits electromagnetic waves (primary field) at a certain frequency, which leads to induction of eddy currents in any conductive layer beneath the instrument. These eddy currents induce again an electromagnetic field (secondary field), which is measured together with the primary field by a receiver coil. Because of induction processes, the secondary field has a phase shift to the primary field. This phase shift together with the strength of the secondary field is a function of the thickness and the conductivity of layers underneath the instrument.

Due to the large conductivity contrast to the saline sea water, the air, snow and ice layer can be assumed to be electrical insulators. With known sea water conductivity (see section 4.2.) the EM signal can be modelled as a function of height above the sea level (Fig. 8).

While the EM system gives the distances from the instrument to the sea surface (under the sea ice), a laser altimeter records the distances to the top of the sea ice or snow layer. The snow plus ice thickness is equal to the laser range minus the EM-derived distance.

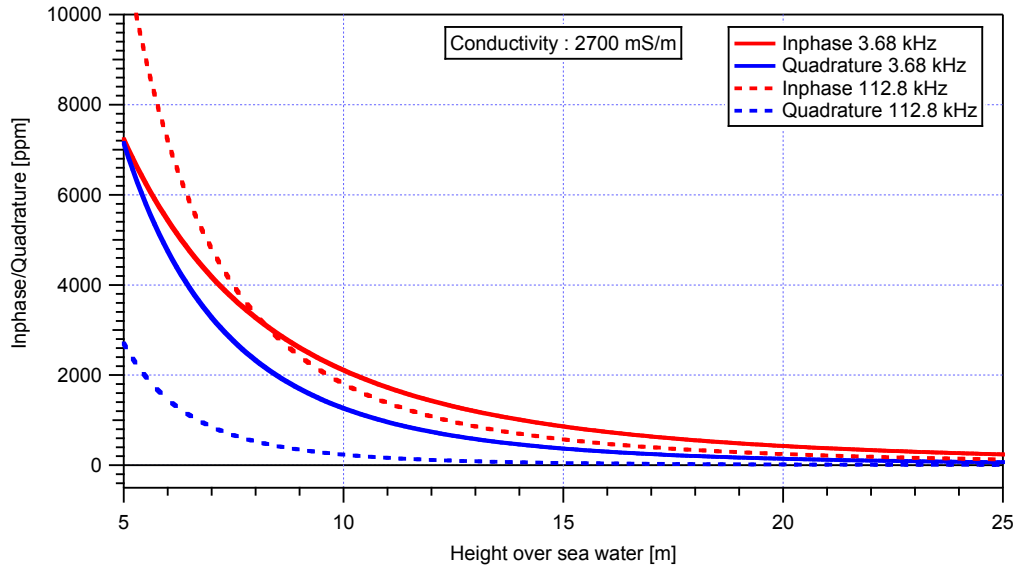


Fig. 8: Forward model results for inphase and quadrature channels (conductivity 2700 mS/m).

4.2. Sea water conductivity

A salt water conductivity of 2300 mS/m was used for data processing.

4.3. Imaging geometry

All aerial pictures were taken with a GPS-compatible Ricoh[®] *Caplio* camera. The external GPS antenna was placed outside the helicopter, approximately 1.8 m (c_x and c_y , Fig. 9) away from the image centre point. The GPS position was taken every second. GPS-heights (h_{GPS}) were corrected using the Bird Laser altimeter (h_{Laser}) plus rope length (approx. 29 m). The used zoom focal length was 5.8 mm. The 35 mm equivalent is 28 mm with a view angle of 46.4° (β - vertical) x 65.5° (α - horizontal). After defining image corner coordinates, photographs were georeferenced to a stereographic coordinate system using a cubic convolution methodology.

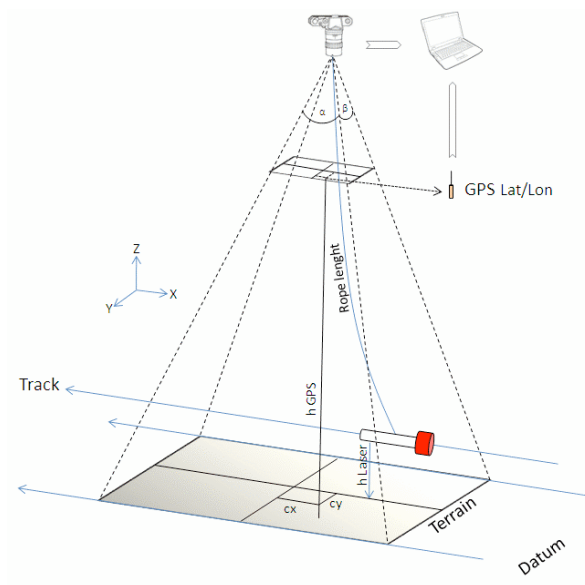


Fig. 9: Imaging geometry of the photogrammetric sea ice survey.

5. Data quality

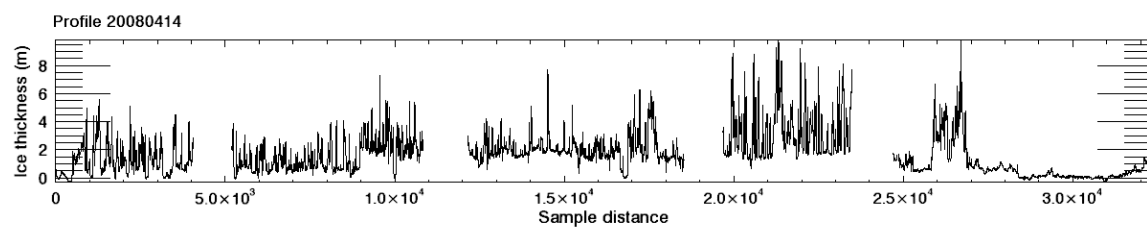
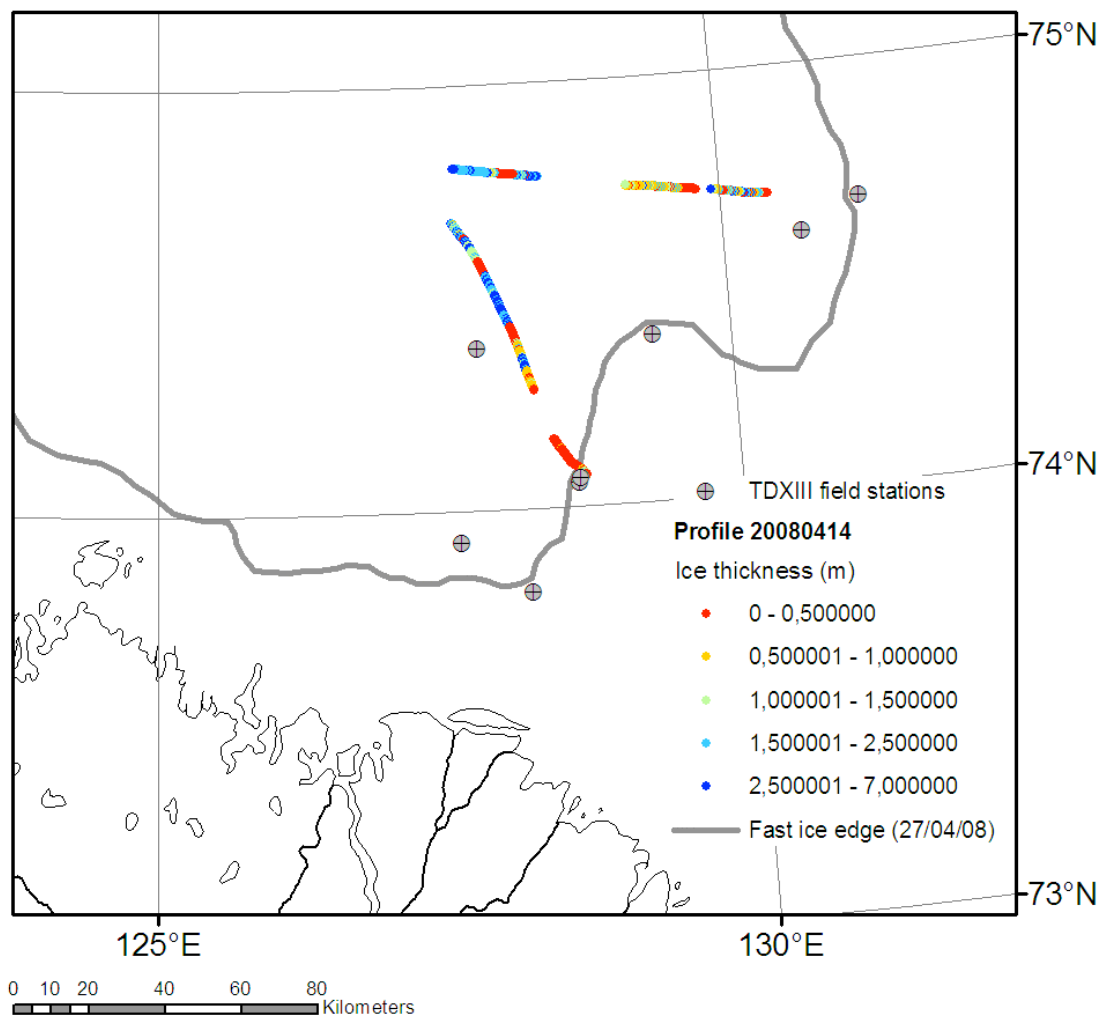
The first flight (April 10) was used to test the connectivity of the instrument to the MI-8 helicopter.

Operations carried out between April 14 and 19 were affected by the unstable power supply in Russian MI-8 helicopters ($> 28V$). Oscillating voltages led to temporary instrument failures and subsequent instrument restarts. Due to the induced temperature-driven drift of the zero level of the instrument, the tracks taken on April 19 are not useable. The tracks taken on April 14 and 16 might contain inaccuracies in an order of ± 10 cm.

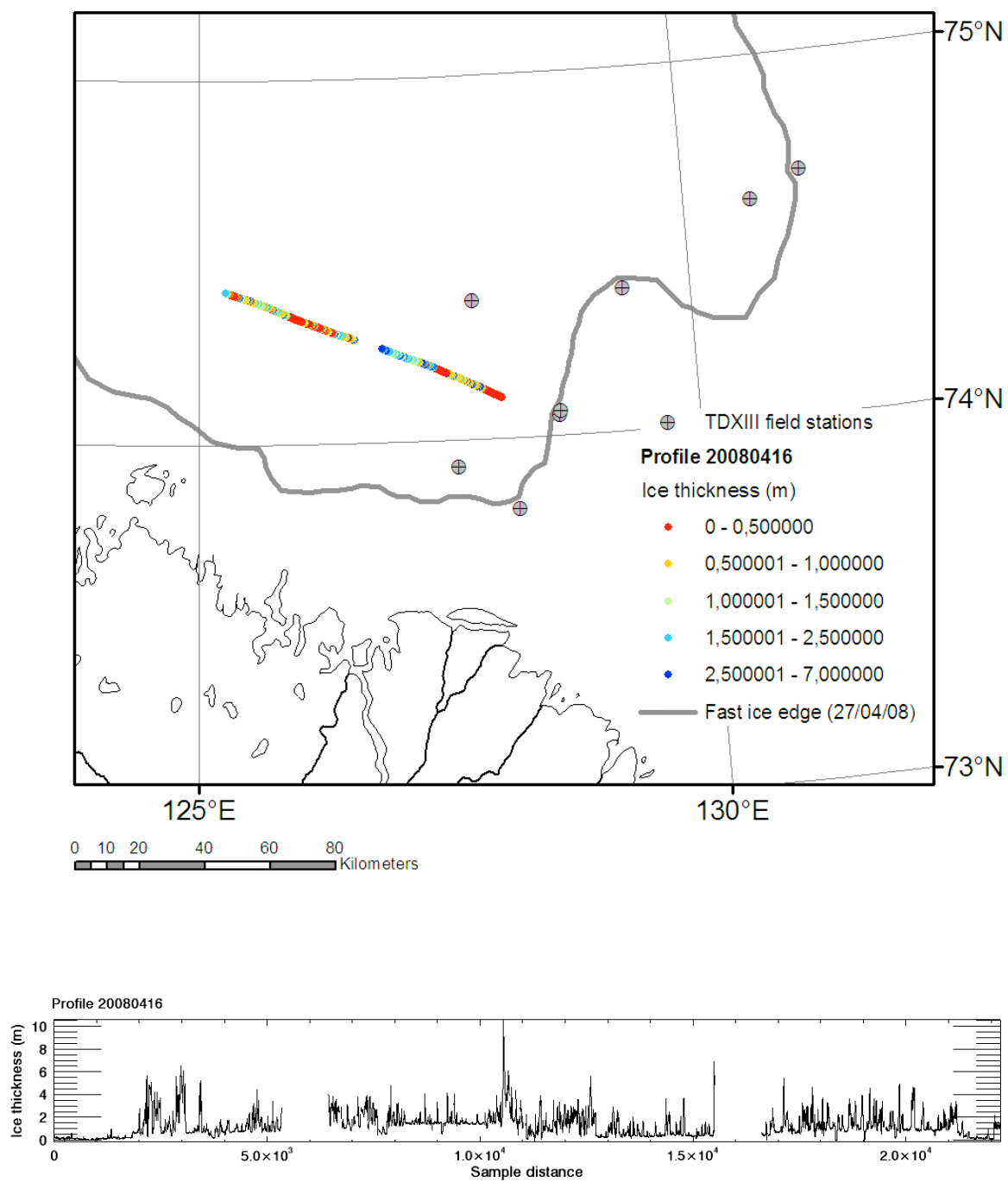
Because of the unstable power supply, the Bird laser altimeter display was unavailable during all flights. In addition, the internal MI-8 helicopter altimeter was not working correctly between 20 and 80 feet. Therefore, the helicopter could not maintain a constant working level. Errors associated to changes in working level have not been corrected so far.

6. List of profiles

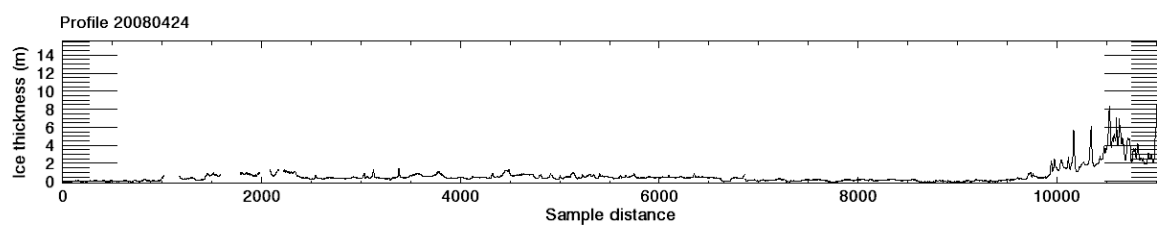
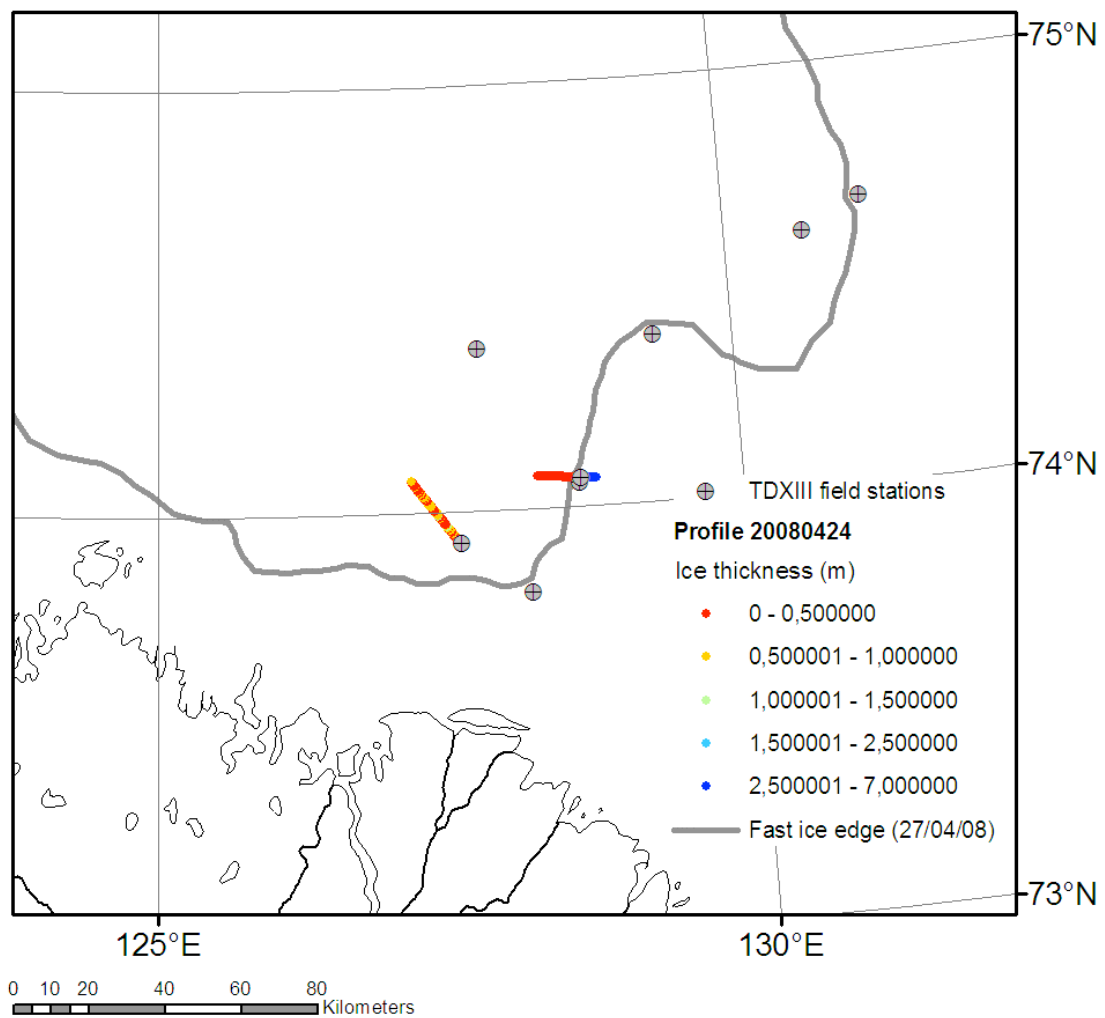
20080414



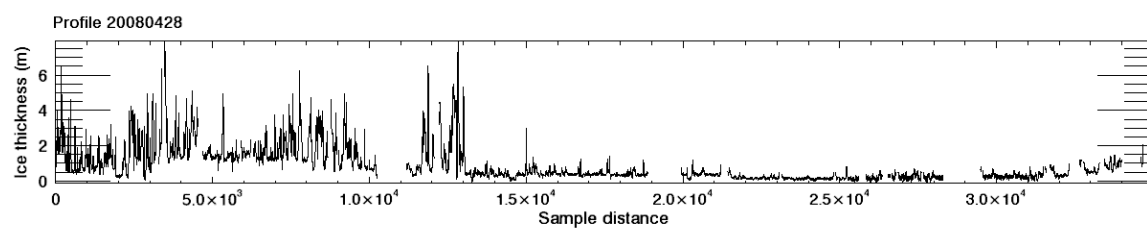
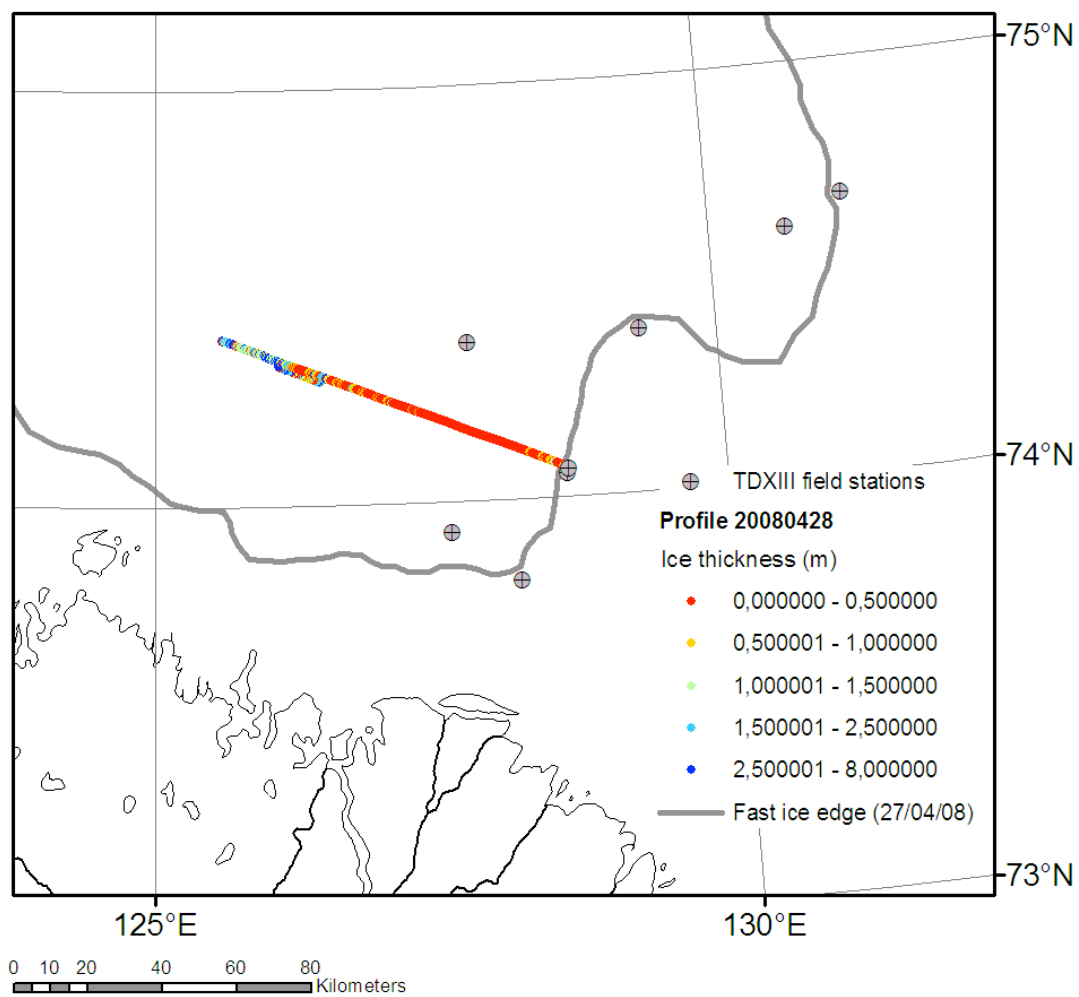
20080416



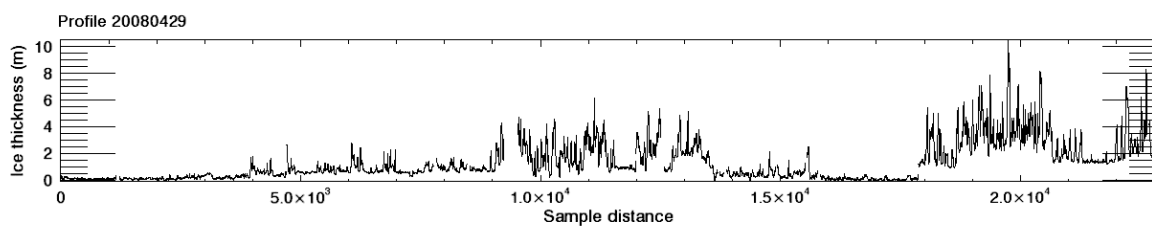
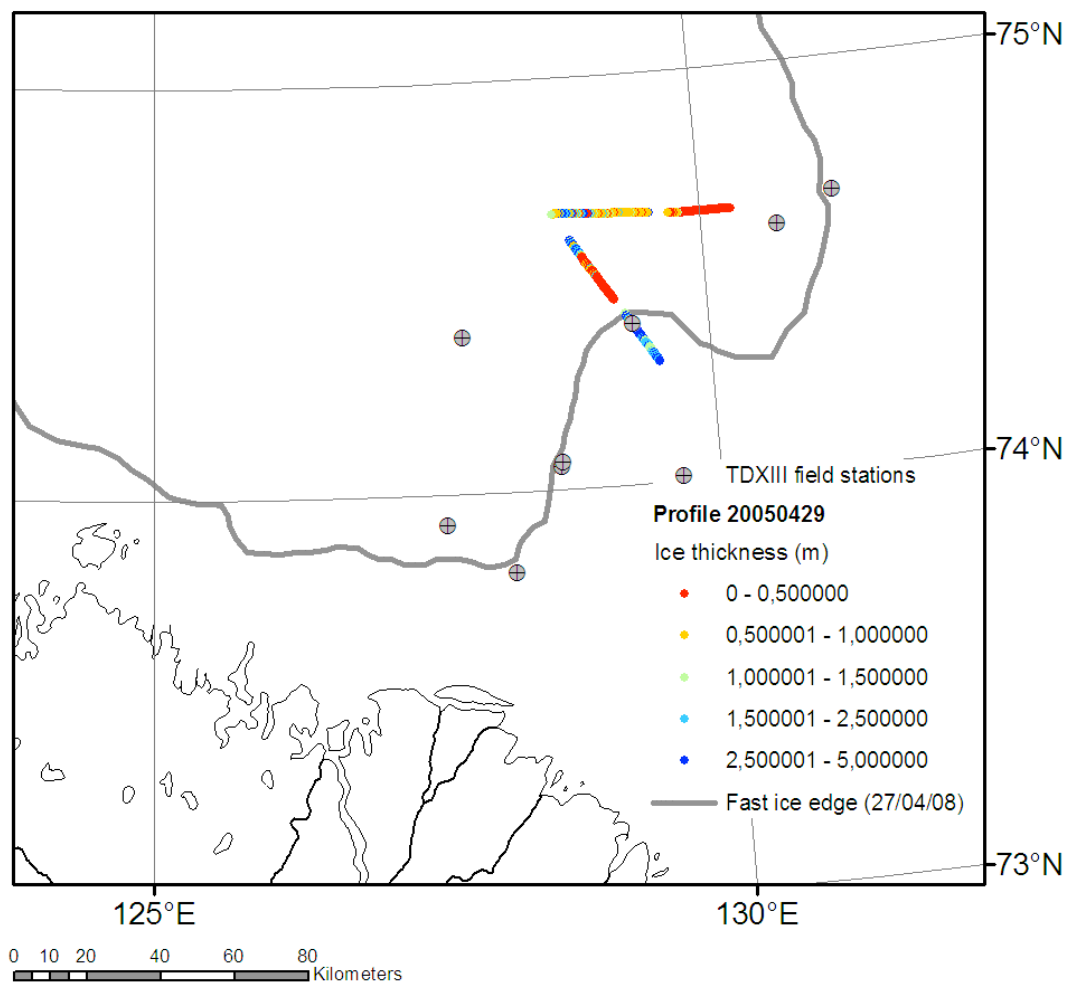
20080424



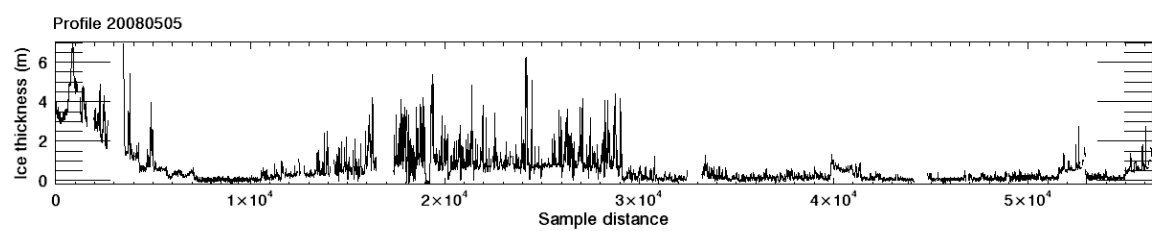
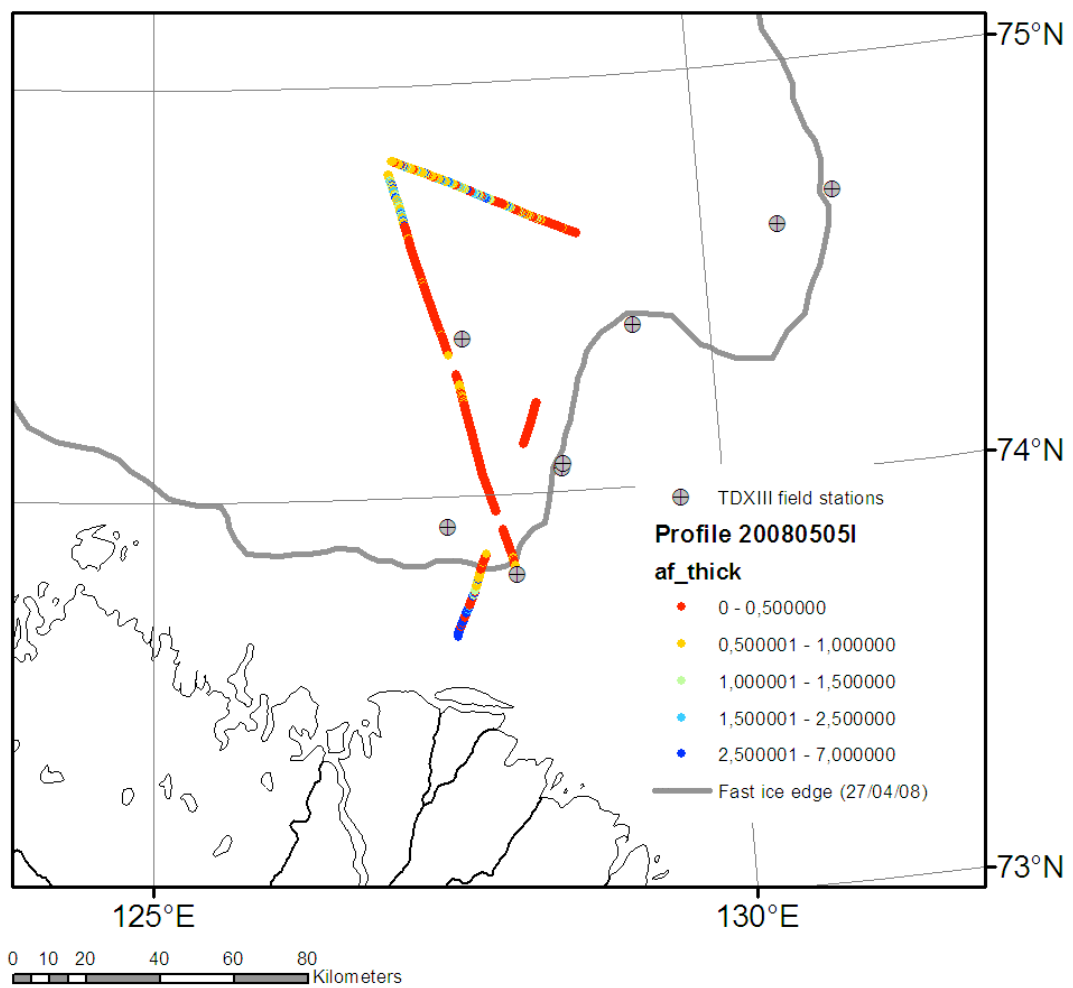
20080428



20080429



20080505



7. Data format

For each profile one data file is delivered. The file naming convention is given by:

\$profile_id_allfinal.dat.

The files are standard ASCII with MS Windows newline format. The first line can be skipped as a header.

Table 3: Allfinal data format.

Column	Format	Unit	Description
af_lat	F12.7	deg	Latitude
af_lon	F12.7	deg	Longitude
af_gps_time	F12.7	hour	Time
af_dist	F12.3	m	Distance since start of profile
af_fid	I9	-	Record number
af_thick	F8.3	m	Sea ice thickness [m]
af_alt	F8.3	m	Laser range [m]

8. Basic formulas

The primary and secondary magnetic field can be described as a harmonic signal with a frequency ω and a phase angle ϕ :

$$\begin{aligned} H_p &= A_0 \cdot \sin(\omega t) \\ H_s &= A_1 \cdot \cos(\omega t - \phi) \end{aligned} \quad (1)$$

where A_0 and A_1 are functions of the geometry of the transmitter/conductor/receiver system. The ratio of secondary to primary field can be separated into a real and imaginary part,

$$\frac{H_s}{H_p} = I + i \cdot Q \quad (2)$$

with I called Inphase and Q Quadrature. These values can be easily converted into amplitude A and Phase ϕ and vice versa via a transformation between cartesian and polar coordinate system:

$$\begin{aligned} A &= \sqrt{I^2 + Q^2} & \phi &= \tan\left(\frac{Q}{I}\right) \\ I &= A \cdot \cos \phi & Q &= A \cdot \sin \phi \end{aligned} \quad (3)$$

Subsequently an amplitude phase correction of I and Q can be performed in polar coordinates:

$$\begin{aligned} I_{corr} &= (A \cdot \Delta A) \cdot \cos(\phi + \Delta \phi) \\ Q_{corr} &= (A \cdot \Delta A) \cdot \sin(\phi + \Delta \phi) \end{aligned} \quad (4)$$

The model curves, which are calculated by a solving a Hankel transformation, are approximated by a double exponential function for each I and Q channel,

$$[I|Q]h = c_0 + c_1 \cdot e^{-c_2 h} + c_3 e^{-c_4 h} \quad (5)$$

where h is the height of the instrument above the conductive water layer. For a given I or Q a simple inversion of equation (5) results in the EM derived distance to the conductor h_{em} .

Finally the snow plus sea ice thickness can be obtained by subtracting the laser range d_{laser} from this distance:

$$z_{ice+snow} = h_{em} - d_{laser} \quad (6)$$

ICE PHYSICS INVESTIGATIONS

K. Tyshko

State Research Center – Arctic and Antarctic Research Institute, St. Petersburg, Russia

1. Introduction

Investigations of ice crystal structure and the physical and mechanical properties of sea ice in the Laptev Sea nearshore area carried out during previous joint Russian-German expeditions revealed specific stages in sea ice cover formation dependent on the hydrometeorological regime of the basin. Ice crystal structure is highly variable in this area due to changeable dynamic conditions during sea ice freeze-up, such as variability of currents of different velocity and direction together with sharp temperature and salinity oscillations. In the southern Laptev Sea, ice structure and the physical and mechanical properties of sea ice are strongly affected by freshwater runoff as sea ice of different salinity range is formed. The distribution of the freshwater lens in the flaw polynya and beneath the sea ice cover causes overcooling of both surface water layer (due to heat loss) and pycnocline layer (due to convection induced by double-diffusion). Intensive mixing of fresh- and seawater produces crystals of frazil ice directly in the mixing layer (due to concentration). Frazil ice and shuga can drift for dozens of kilometers from their source region, thus affecting the crystal structure and physical characteristics of pack ice (Tyshko and Kovalev, 2006).

During spring time, an evident crystal alignment was observed in the basal fast ice layers formed under the influence of steady surface currents. This physical property is characteristic of the sea ice cover in many Arctic seas. Crystal optic analysis of the whole ice sequence reveals the fact that the surface currents are stable during the whole ice formation period (Dmitrenko et al., 2002).

Considerable temporal variability of the structure and main physical properties of sea ice observed during spring time are caused by thermometamorphism resulting from radiational and conductive heating accompanied by the processes of inner and surface melting, weakening and destruction of ice. Knowledge about the mechanisms of these processes and the timing of ice transformations from one genetic type to another is essential for practical activities with the use of sea ice as a natural platform (Frolov and Gavrilov, 1997).

During the POLYNIA 2008/TRANSDRIFT XIII expedition there was a good chance to continue investigating these processes. The program of ice physics investigations included the following research tasks:

- to investigate the role of frazil ice and shuga in the processes of ice formation and the formation of its crystal structure during fall/winter and the first half of spring, when ice of both types is intensively formed in the open water of the polynya zone;
- to investigate the development of crystal alignment (C-axes of crystals) under the effect of steady surface currents;
- to describe the spatial variability of ice crystal structure and physical properties of sea ice in dependence of the regionally dominant processes of sea ice formation;
- to reveal regional peculiarities of the temporal variability in the structure and physical properties of sea ice under the influence of the processes of dynamo- and thermometamorphism.

2. Instruments and methods

Ice temperature was measured by Hanna electronic thermometer Checktemp 1 with a re-

solution of 0.1°C and laboratory mercury thermometers TL-4 with the scale of 0.1°C and the accuracy of 0.05°C. Ice salinity was measured by WTW instrument Cond 315i/SET with the resolution of 0.1‰. Ice texture was visually analyzed in the drilled ice cores. For this purpose a vertical plate with the thickness of 1.0-1.5 cm was cut out from every core. Analysis included description of textural layers and all inclusions together with their dimensions. Investigations of ice structure were carried out in the cold laboratory in Tiksi using a polarizing table which consisted of two parallel polaroids lighted from below. Vertical and horizontal ice blocks with the size of 12x9x1.0-1.5 cm were cut out from various layers of the ice cores, and thin sections were prepared. The thickness of these sections was 1-3 mm as it should not exceed the size of crystals. The sections were placed between the polaroids for making films and prints (Fig. 10).

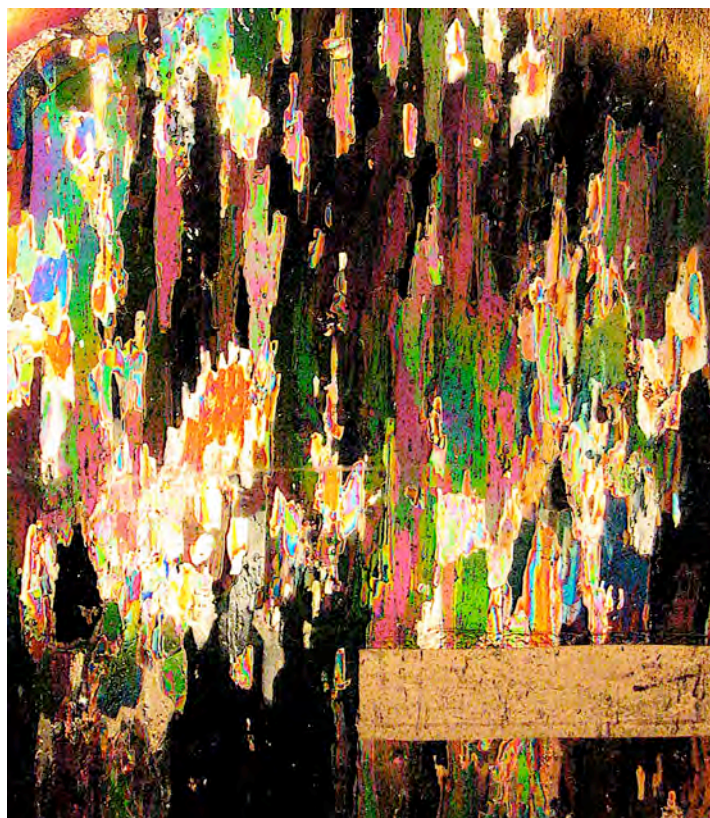


Fig. 10: An example of an ice crystal structure seen under polarized light.

3. Main results

During the 2007-2008 winter season the sea ice cover near the Laptev Sea flaw polynya developed under an intensive dynamic influence as evidenced by frequent changes of structural layers in the ice cores. Textural and structural analyses showed that the growth of fibrous crystals typical for fast ice developing under stable and calm conditions was periodically interrupted by advection of snow, shuga and frazil ice crystals beneath the ice cover. In such cases the subsequent growth of sea ice went on as adfreezing of these layers (Fig. 11). At some ice stations such events occurred very often (Fig. 12).



Fig. 11: Small-grained ice crystal structure in the lower layer of the sea-ice cover.

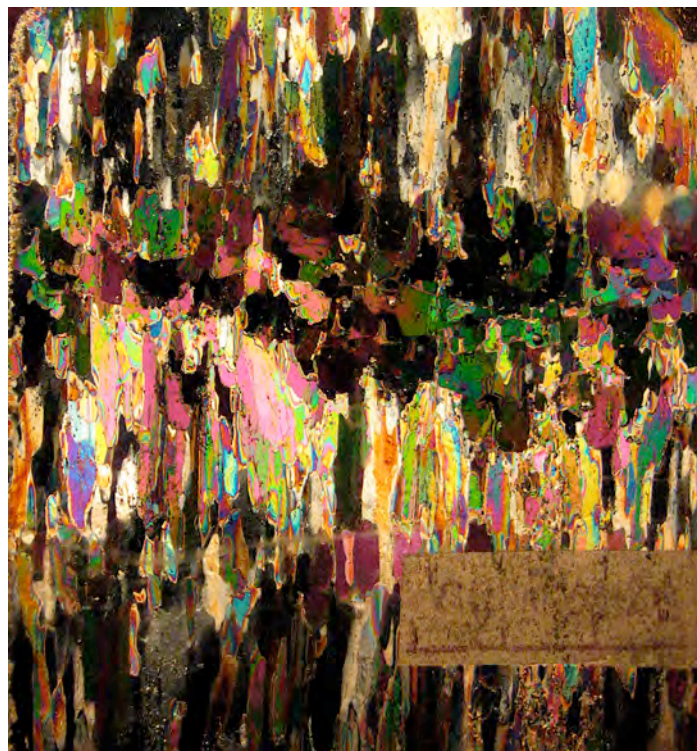


Fig. 12: Layered ice structure.

Under the dynamic influence the ice floes suffered periodical compression. This resulted in the formation of pressure ridges and rafted or layered ice and metamorphic transformations of ice crystals. Depending on the strength of the external forces three main types of metamorphic transformations of ice crystal structure could be distinguished. At low compression strength the ice crystals were subject to plastic deformation which developed as a process of inter-

granular shifts of basal plates parallel to each other. This resulted in the appearance of crystals with irregular forms including U-shaped ones (Fig. 13). As compression strength increased, not only the basal plates but the whole crystals started to move along each other thus producing a wavy structure (Fig. 10, 14). When compression strength reached 40-50% of its critical value (when ice is broken), deformation of crystals acquired elastic-plastic form. In such cases the inclined bended fibrous crystals were broken, and small ice pieces shifted in the direction of applied strength making the crystals longer in the horizontal plane (Fig. 15). The most common type of dynamometamorphic transformations was fragile destruction of the ice crystals under a compression strength reaching 70-80% of its critical value. In these cases the ice structure represented a mass of very small crystal pieces without any expressed edges (Fig. 16) (Tyshko, 2007).

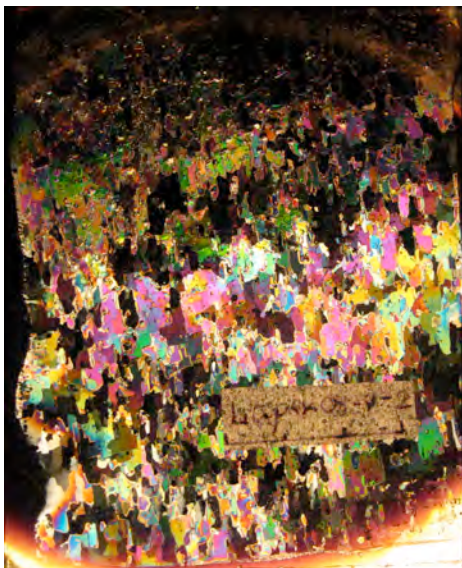


Fig. 13: Plastic intergranular deformation of ice crystals.

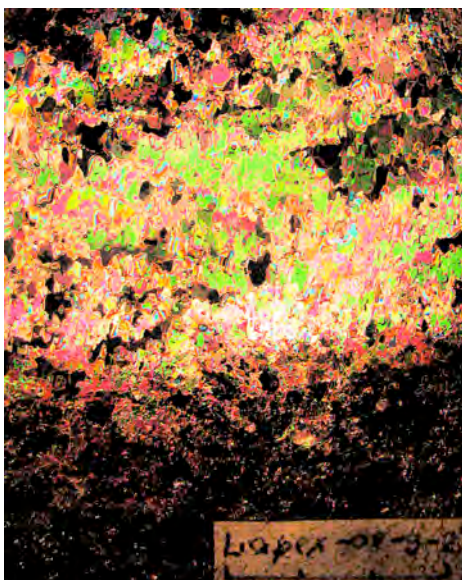


Fig. 14: Plastic inter-crystal deformation of ice crystals.

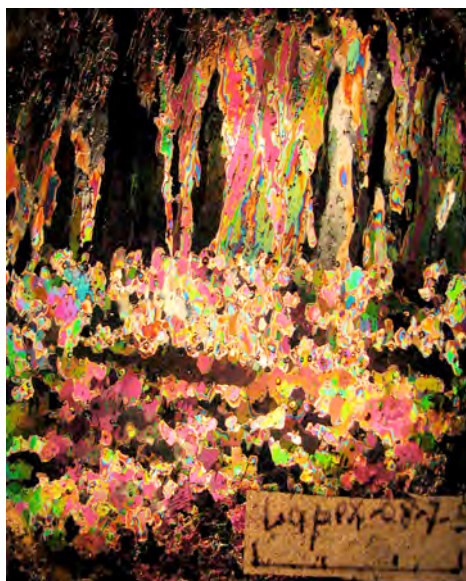


Fig. 15: Elastic-plastic deformation of crystals.

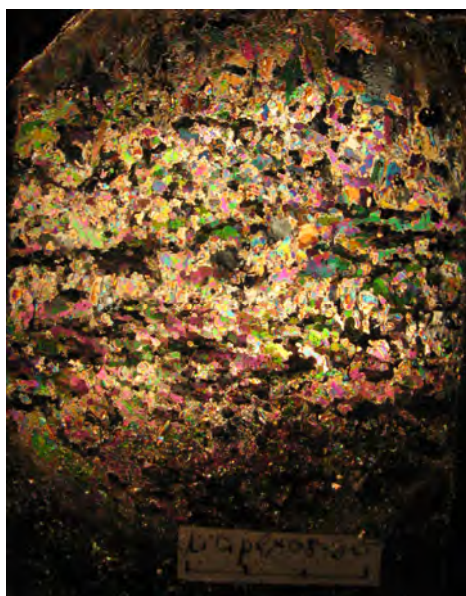


Fig. 16: Fragile destruction of ice crystals with formation of shapeless groups of very small pieces.

The results of ice physics investigations partly support the data obtained in previous expeditions. However, there are certain differences because of different hydrometeorological conditions during ice formation. This primarily concerns intensive radiational heating of the ice cover expressed by the basal ice layer temperature being higher than the surface water temperature. Like in April 1999, their maximum difference reached $0.8-0.9^{\circ}\text{C}$ with the ice thicker than the equilibrium thickness at a given air temperature. In this expedition this was the ice thickness of 145 cm.

In April 1999, at almost all ice stations we observed a clearly expressed alignment of the main optical axes of crystals in the horizontal plane (C-axes) following the directions of the steady surface currents. This year such a phenomenon was not typical because of repeated interruptions of the orientated vertical growth of fibrous crystals by formation of layers with small grained crystals of frazil ice and shuga. This year alignment was recorded at only two stations (Fig. 17A, st. 1, layer 60-62 cm; Fig. 17B, st. 4, layer 53-55 cm).

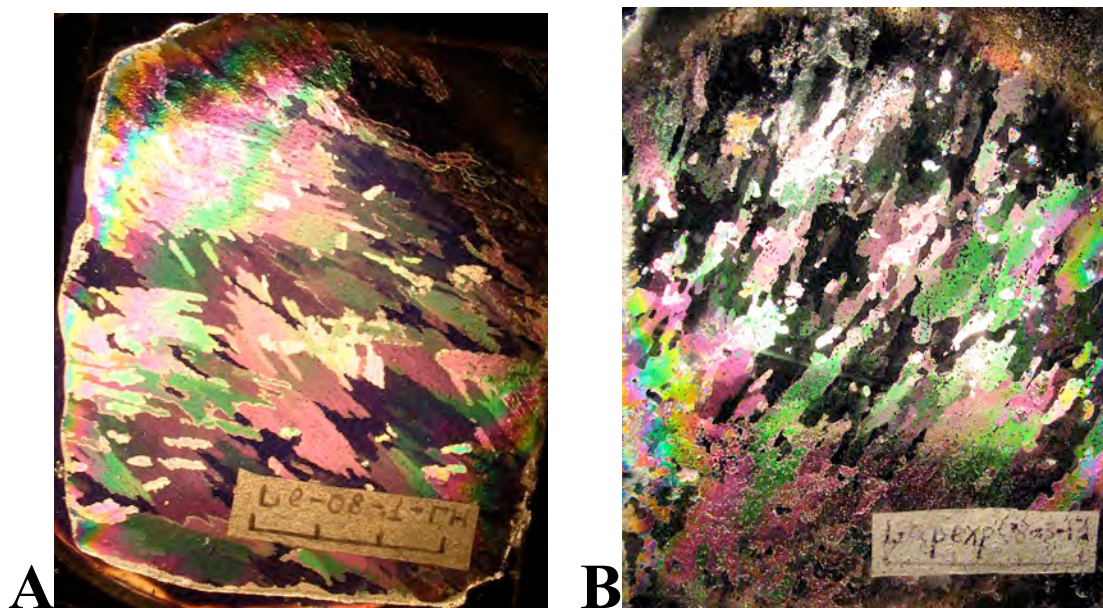


Fig. 17: A – spatial alignment of crystals on a horizontal ice section (2008, st. 1, layer 60-62 cm); B – spatial alignment of crystals on a horizontal ice section (2008, st. 4, layer 53-55 cm).

The intensity of brine discharge, which is the basic carrier of all inclusions in the ice cover towards its basal layer, strongly depends on the layered crystal structure of the ice cover. Maxima of sea ice salinity are observed in shuga layers, and minima in fibrous ones (Lyalyagin and Tyshko, 2002).

OCEANOGRAPHIC INVESTIGATIONS

S. Kirillov¹, I. Dmitrenko², M. Makhotin¹, T. Klagge², J. Hoelemann³

¹State Research Center – Arctic and Antarctic Research Institute, St. Petersburg, Russia

²IFM-GEOMAR, Leibniz Institute of Marine Sciences, Kiel, Germany

³Alfred Wegener Institute for Polar and Marine Research, Bremerhaven, Germany

1. Goals and research tasks

The aim of the oceanographic research activities during the expedition was to investigate the influence of the open water areas (polynyas) on the thermohaline and dynamic regimes of the Laptev Sea shelf waters during winter. The research tasks were:

- to carry out oceanographic measurements together with hydrochemical and biological sampling on the fast ice edge (15 stations) and the drift ice (2 stations);
- to make 1-1.5 km long oceanographic profiles across the fast-ice edge with 150 m intervals between observational sites;
- to deploy 5 sub-ice oceanographic stations at the fast ice edge during the expedition.

2. Oceanographic equipment

The following equipment was used:

- 2 CTD probes SeaBird 19plus produced by Sea Bird Electronic (USA) with the main sensors measuring temperature, electrical conductivity and pressure; and additional sensors for dissolved oxygen, turbidity and chlorophyll. Main characteristics of the CTD probe:

operational depth:	7000 m
temperature measurement range:	-2 to +40 °C
salinity measurement range:	0-40 ‰
temperature measurement accuracy:	±0.005 °C
salinity measurement accuracy:	±0.001 ‰
triggering time:	4 sec -18 hours
vertical resolution:	from 0.1 m
- 9 probes SeaBird 37 Sea Bird Electronic (USA) with temperature and conductivity sensors (some probes were additionally equipped with pressure sensors). Main characteristics:

operational depth:	7000 m
temperature measurement range:	-5 to +35 °C
temperature measurement accuracy:	0.002 °C
electrical conductivity measurement range:	0.001-7.0 cm/m
electrical conductivity measurement accuracy:	0.0003 cm/m
- 5 acoustic current meters ADCP Workhorse Sentinel 300 kHz. Main characteristics:

operational depth:	200 m
velocity measurement range:	-5 to +5 m/sec
velocity measurement accuracy:	0.5% + 0.5 cm/sec
current direction measurement accuracy:	± 2°

During the expedition 5 sub-ice bottom stations were successfully deployed and recovered. The structure of such a station is shown in Fig. 18.

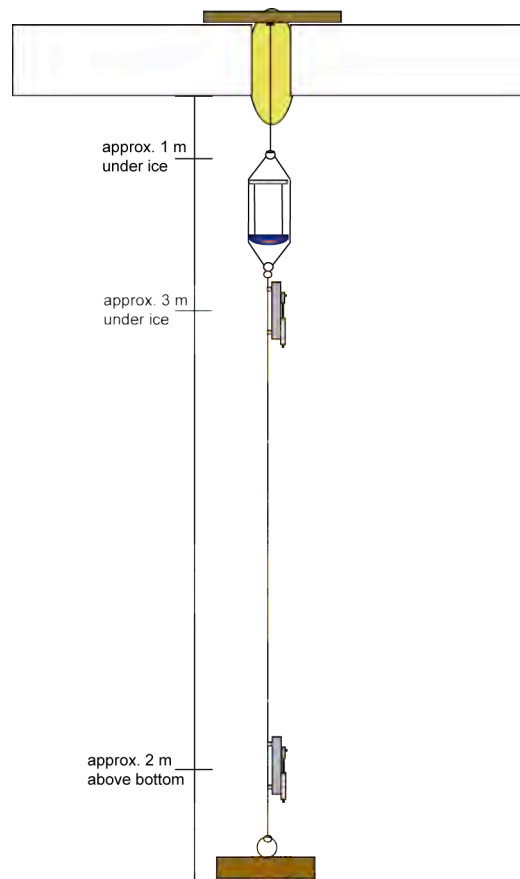


Fig. 18: General scheme of deployed sub-ice bottom station.

3. Methods

Vertical CTD measurements were carried out from fast or drift ice in the close vicinity of the polynya. Holes in the ice were drilled by a motor drill. In order to reduce the error of measurements caused by ice crushing during drilling and sensor cooling under low air temperatures, the CTD probe was kept for some time under ice, and the measurements were taken repeatedly.

CTD measurements were carried out before the deployment of the sub-ice bottom stations in order to determine water depths at the sites and the depth for fixing the instruments. The latter depended on the main or seasonal pycnocline position, presence of warm intermediate water layer or bottom layer of warm water advected with reversed currents. Later, the load and the rope with the fixed instruments were run in a special hole of a bigger diameter. The upper end of the rope was fixed on the ice surface. To protect the hole from freezing, a special balloon was mounted there, which, after being filled with air, occupied it completely. The station recovery was made with the help of a special tripod fixed above the hole.

4. Activities

In total, 60 CTD measurements were carried out at 17 oceanographic stations (Fig. 19). Five sub-ice bottom stations were deployed and successfully recovered (at the sites of the oceanographic stations 01, 02, 04, 05 and 08).

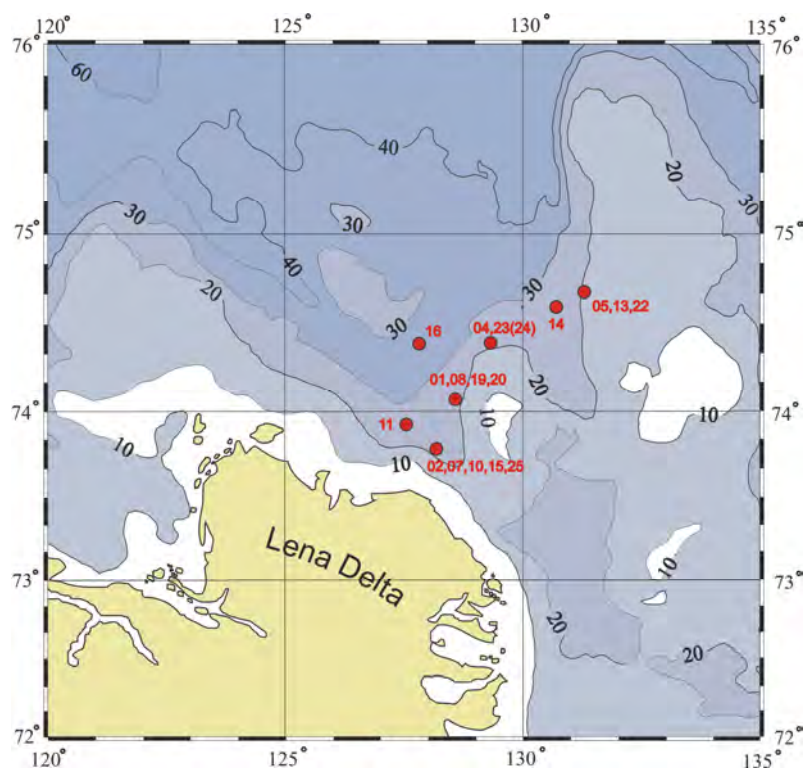


Fig. 19: Location of oceanographic station sites, POLYNYA 2008/TRANSDRIFT XIII expedition.

5. Preliminary scientific results

To investigate the influence of the polynya on the hydrophysical and hydrodynamic properties of the Laptev Sea shelf waters, CTD profiles were made across the fast ice edge in both directions, onshore and offshore towards the open water (on the newly formed thin ice). To reveal the temporal variability of these characteristics, the measurements were repeated several times during the expedition.

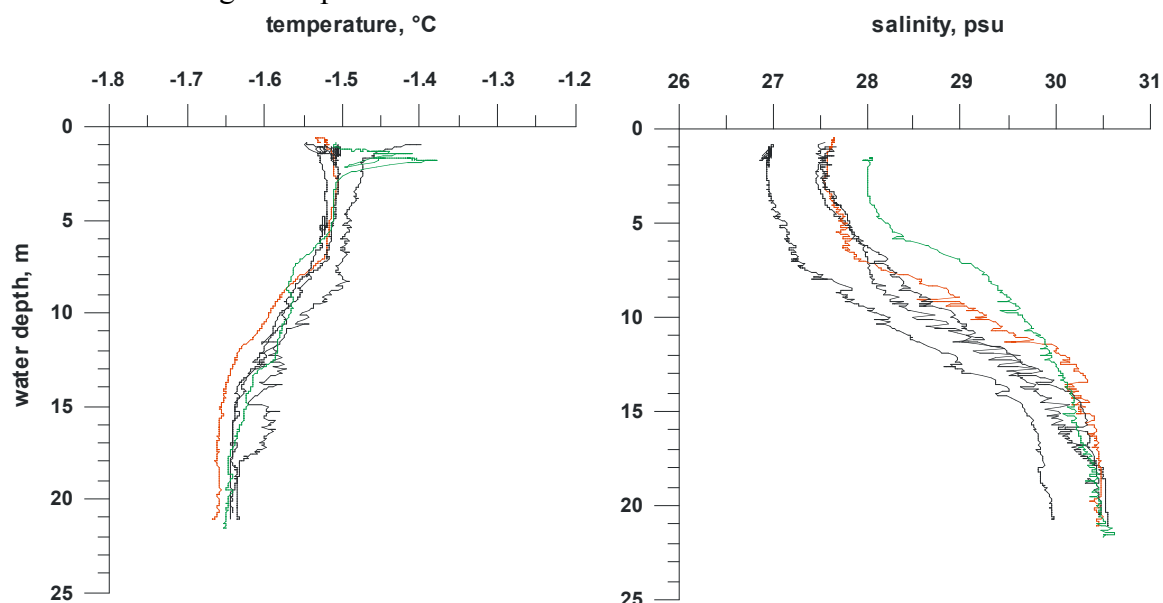


Fig. 20: Vertical distribution of temperature and salinity at station 02 (11.04.08); black lines correspond to profiles made from the fast ice edge towards the shore; red lines correspond to profiles made from the fast ice edge towards the open water (on the newly formed ice); the green line corresponds to the profile made on the fast ice edge on 14.04.08.

The data obtained do not show any regular changes in the hydrophysical water properties along the offshore transect from the fast ice edge. Figure 20 demonstrates small temperature and salinity differences between the profiles made at the same station, which are rather a result of measurement errors due to low air temperatures than due to polynya influence. Most likely, polynya processes were weak during the expedition period because of predominantly northerly winds favouring polynya closure.

The records of the sub-ice bottom stations reveal a considerable influence of the tidal component on the temporal variability of both temperature and salinity (Fig. 21).

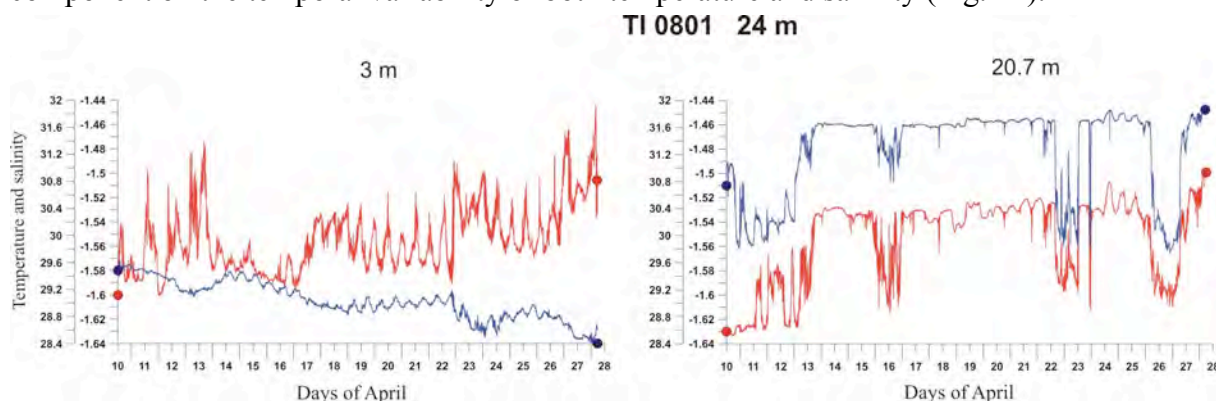


Fig. 21: Temporal variability of temperature (red line) and salinity (blue line) at station 01. Left panel – 3 m water depth, right panel – 21 m water depth.

The influence of polynya processes is well manifested in the data from station 02 (Fig. 22). For instance, on April 26, a sharp drop of subsurface temperature to a temperature close to freezing point was accompanied by a simultaneous salinity rise by more than 4 psu. Most likely, during the period between April 26 and 30 the station came under open water conditions, which caused water cooling by convective mixing and salinity rise due to active ice freeze-up.

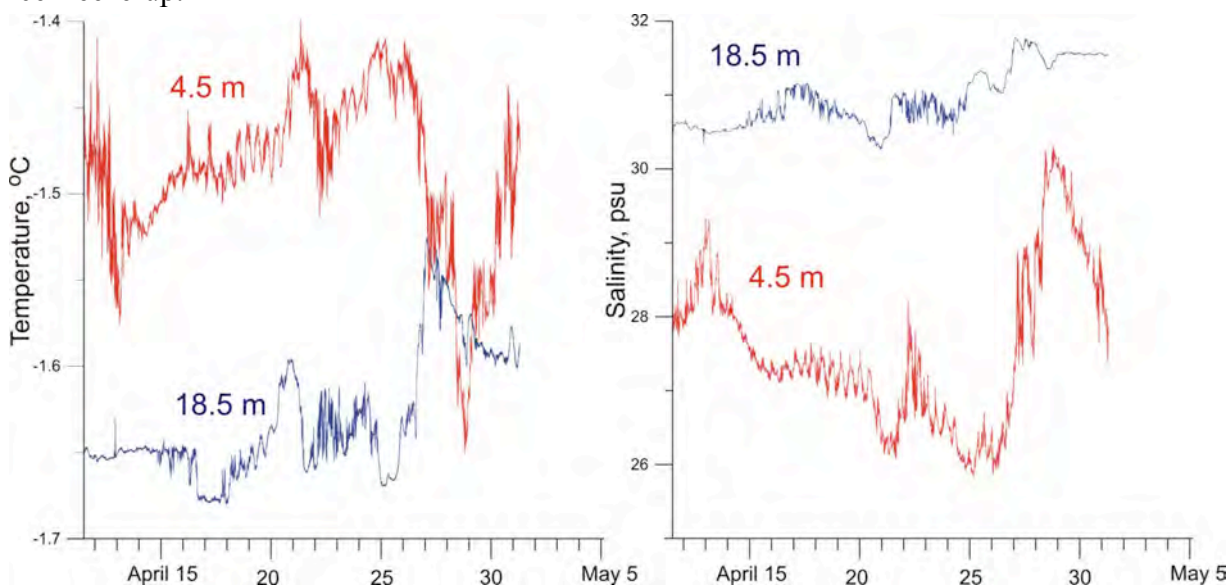


Fig. 22: Temporal variability of temperature (left panel) and salinity (right panel) at station 02. Red line – 4.5 m water depth, blue line – 18.5 m water depth.

During the expedition we recorded the occurrence of a warm and saline bottom water layer overlain by a layer with high temperature and salinity gradients. Such a phenomenon has often been recorded on the Laptev Sea shelf. This is a result of onshore advection of relatively

warm and saline open sea waters from the continental slope which represent Atlantic-derived waters transformed by intermixing with shelf waters. The vertical temperature and salinity distributions at station 14 on April 21 show a temperature rise by 0.2°C and salinity rise by 1 per mill in the bottom water layer (Fig. 23).

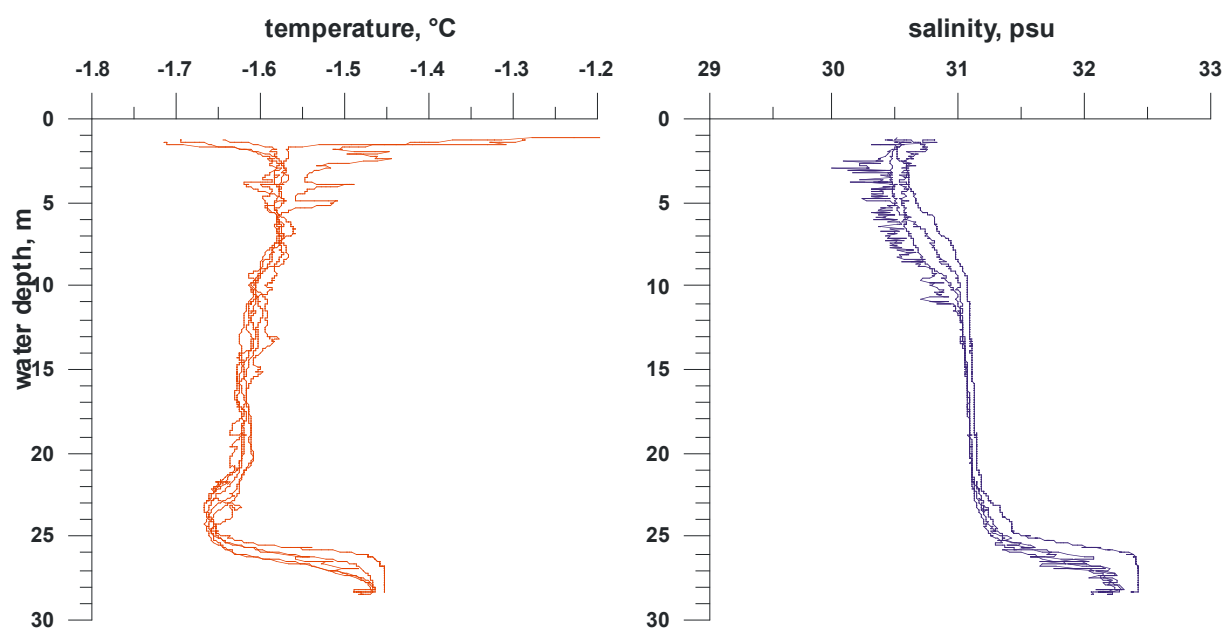


Fig. 23: Vertical distribution of temperature and salinity at station 14 (21.04.08).

FIRST USE OF A FREE-DRIFTING PROFILING FLOAT (NEMO) IN THE LAPTEV SEA POLYNIA

T. Klagge¹, J. Hoelemann²

¹IFM-GEOMAR, Leibniz Institute of Marine Sciences, Kiel, Germany

²Alfred Wegener Institute for Polar and Marine Research, Bremerhaven, Germany

Polynyas are characterized by a high heat flux from the water column to the atmosphere, which leads to ice formation and changes of the salinity and temperature fields in the water column beneath the polynya. A detailed description of the salinity and temperature changes during polynya events should lead to a better understanding of the physical processes, like ice formation and mixing, within the polynya. Although oceanographic observations from the polynya are essential, the data acquisition from polynyas is still a challenge.

During the Expedition TRANDRIFT XIII a free-drifting profiling float (NEMO) was used for the first time in an Arctic shelf polynya. Floats are routinely used in “deep water” oceanography. For the deployment in the Laptev Sea the buoyancy system of the float was changed, so that it could operate in shallow and ice-covered water with salinities down to 23 psu. In contrast to a remotely or autonomous underwater vehicle a float is passively moving with the currents. By changing the buoyancy of the system with an internal pump the float profiles a 30m deep water column within 30 minutes. After profiling it emerges and transmits the data together with the GPS position to the observer. The design of the float was changed in such a way as to allow the system to emerge only under open water conditions.

The NEMO float itself is 2.4 m long and approx. 20 cm in diameter. It was produced by “Optimare Sensorsysteme” in Bremerhaven, Germany. It is equipped with a sensor for measuring conductivity, temperature and pressure (SBE41 from Seabird Electronics, Inc.). Most of the remaining parts of the float consist of the buoyancy and telemetry system, the batteries as well as the IRIDIUM satellite transmitter with its antenna, and a GPS device (Fig. 24).

Technical details

- Serial number: 062
- Memory: Flash-memory
- Size (complete length with sensors and antenna): 240 cm
- Profile Pressure (maximum depth): 60 dBar
- Transmission time: 30 minutes
- Ascending speed: approx. 0.08 m/s
- Surface detect temperature: -3.000 °C
- Minimum surface salinity: 23.000 psu
- Batteries float controller: 7.2V / 26 Ah
- Batteries hydraulic, pneumatic and transmitting: 14.4 V / 78 Ah
- Transmitting system: Iridium Short-Burst-Data (SBD), max. message size: 205 bytes

Sensors

The NEMO-float is equipped with a CTD SBE41:

- CTD serial number: 41-3298
- CTD Firmware Version: 2.6
- CTD Sample interval: 1 Hz
- Sensor for Conductivity: Standard Seawater 0.005 psu equivalent
- Sensor for Temperature: ITS-90, accuracy 0.002°C
- Sensor for pressure (depth):
 - Pressure Type: Druck
 - Pressure Range: 2000 dBar
 - Pressure Serial number: 2402599



Fig. 24: NEMO float deployed in the Laptev Sea polynya on April 5, 2008.

Deployment during TRANSDRIFT XIII

During the expedition TRANSDRIFT XIII the NEMO float was deployed at 73° 50.321 N, 128° 06.755 E on April 5, 2008 06:52 UTC. The NEMO float was prepared for deployment and adapted to the local conditions (air temperature, GPS correction, surface salinity, water temperature). After that a test message was transmitted through the satellite system and was successfully received by us. Finally the NEMO float was deployed from the fast ice-edge (Fig. 25). After the data transmission test no data transmission was recorded because currents

pushed the float under the ice where it drifted for the whole two-week period of measurements without emergence.



Fig. 25: Deployment of the NEMO float on the fast ice edge.

HYDROCHEMICAL OBSERVATIONS

A. Novikhin

State Research Center – Arctic and Antarctic Research Institute, St. Petersburg, Russia

1. Introduction

High-latitude ecosystems are especially sensitive to the impact of global warming. It causes a decrease of the sea-ice cover. It also leads to an enhanced influence of Atlantic waters on the Arctic Ocean (Schauer et al., 2002) and the Siberian shelf seas, thus affecting the intensity of hydrochemical and hydrobiological processes (Smagin and Novikhin, 2007). The Laptev Sea is under the strong influence of river runoff. Hence, variations in river discharge determine the distribution of the hydrochemical parameters of seawater (Smagin et al., 2003).

The surface water mass distribution depends on surface current and ice drift patterns formed by changes in atmospheric circulation. In the shallow Arctic seas convective and wind mixing translate these changes to deeper structural levels. This is essential for the functioning of ecosystems in polynya regions.

In order to understand the processes operating in the Laptev Sea polynya and the influence of global climate change on the hydrochemical structure in polynyas, the hydrochemical field investigations during the POLYNYA 2008/TRANSDRIFT XIII expedition concentrated on the following tasks:

- investigating the spatial and temporal distribution of hydrochemical parameters in the river-affected zone;
- investigating the water mass structure in the Laptev Sea polynya region;
- assessing the influence of global climate change on the hydrochemical water structure of the sea and hydrochemical and hydrobiological processes in its polynya region;
- investigating the seasonal and multiannual variability in the distribution of hydrochemical parameters.

2. Equipment and methods

Water samples were collected with 5-liter plastic bathometers. The samples for oxygen concentration were taken first. Water was sampled into 100-ml glass bottles. After sampling, oxygen was fixed by sequential adding of 1 ml of manganese chloride and 1 ml of potassium iodide/sodium hydroxide solution. The sample was mixed until an evenly distributed residuum was formed. After precipitating, it was dissolved by addition of 2 ml of sulphuric acid. The dissolved oxygen content was determined by titration with sodium thiosulphate using electronic burette following the modified Winkler method.

Water samples for nutrients were collected in 50-ml plastic bottles. Immediately after sampling the bottles were frozen under -20°C and thus later transported to the Russian-German Otto Schmidt Laboratory for Polar and Marine Research for further analysis. The nutrient concentration was measured by the automatic analyzer SKALAR Sun Plus System following the instructions to this device. The procedure includes disintegration of the sample into finest microprobes with the help of air bubbles. Prior to entering the optical dish the sample is colored with gradually added reagents. The nutrient concentration in the samples is then determined by the photocolorimetric method.

The dissolved oxygen content was additionally measured by an SBE-43 sensor installed on the oceanographic SBE19 plus probe.

3. Preliminary results

During the expedition water samples were taken at 15 oceanographic stations in the Laptev Sea polynya region (Fig. 26). In total, 40 samples were analyzed for dissolved oxygen, and 79 samples for nutrients.

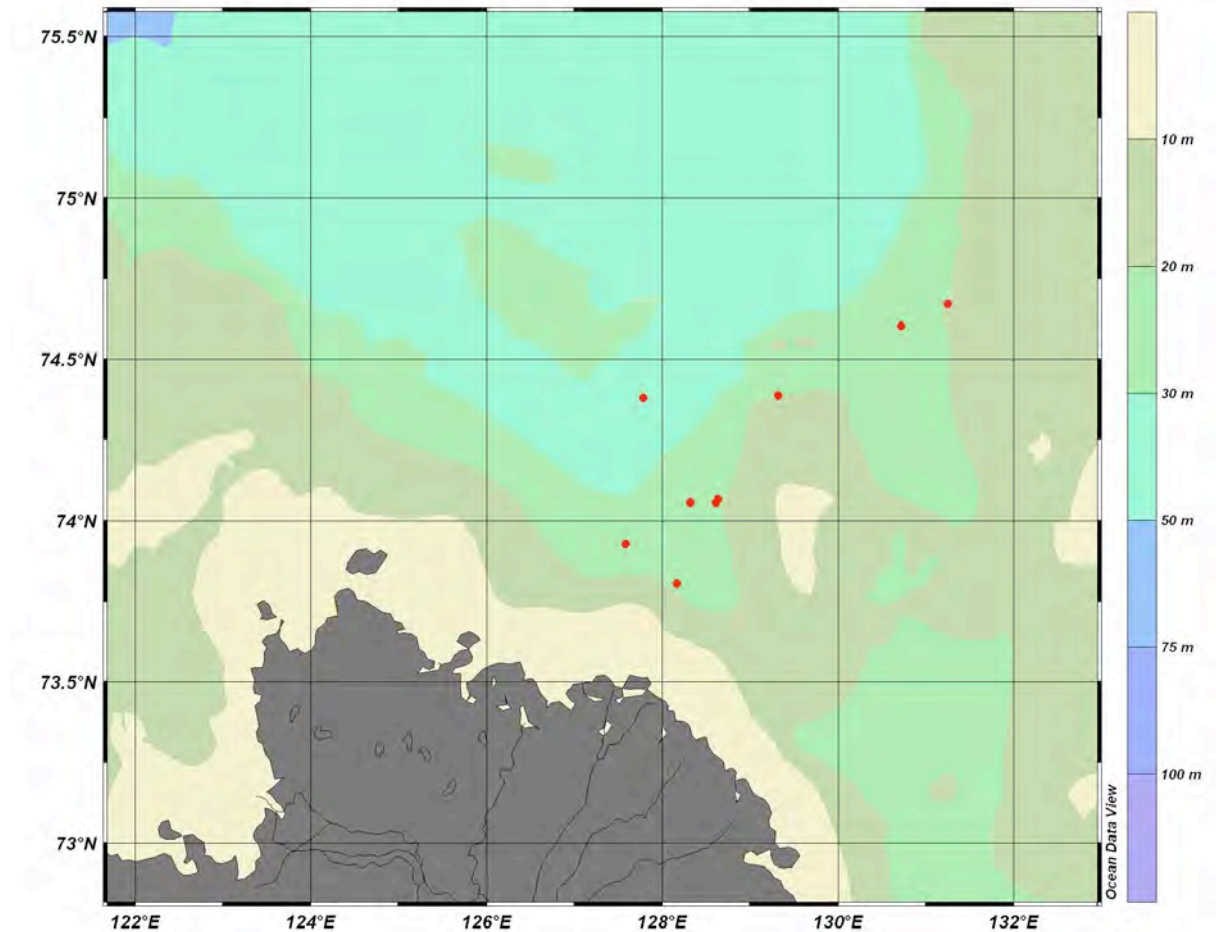


Fig. 26: Water sampling sites during the POLYNYA 2008/TRANSDRIFT XIII expedition.

A preliminary comparison of the data on dissolved oxygen concentration measured by the sensor and by the Winkler method shows that the SBE-43 sensor gives an adequate reflection of the vertical profile (Fig. 27). However, the results obtained by the sensor require correction as they are slightly lower than the values obtained by the Winkler method. As there is a certain sensor lag, when correcting the data it is necessary to consider both the measurements taken on the way down and up. Despite some limitations of the sensor it allows tracing the fine structure of the vertical distribution of dissolved oxygen, which is impossible to reveal when analyzing profiles obtained in the field.

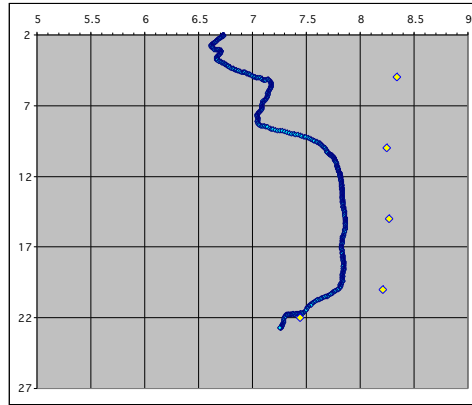


Fig. 27: Vertical distribution of dissolved oxygen obtained by the SBE-43 sensor (blue dots) and by the Winkler method (yellow dots).

The concentration of dissolved oxygen ranges from 5.67 ml/l (bottom layer, station 14) to 8.96 ml/l (5 m water depth, station 19) (Fig. 28). In the northern region (stations 14 and 19) the concentration of dissolved oxygen is relatively low in the bottom water layer.

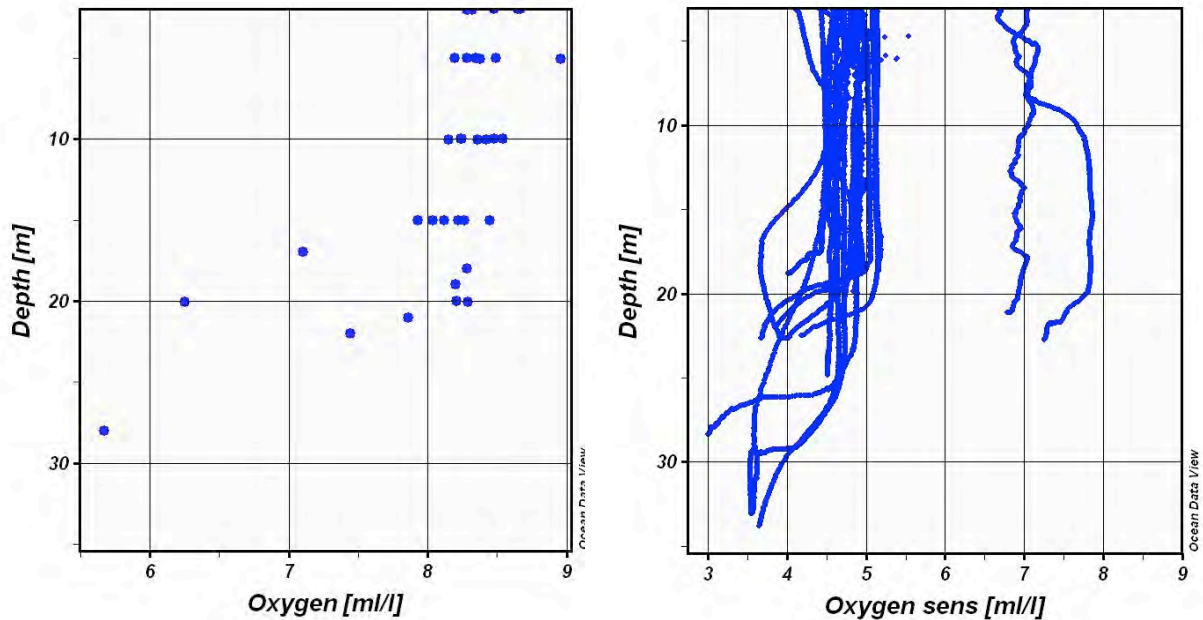


Fig. 28: Vertical distribution of dissolved oxygen. Left panel: Winkler method; right panel: oxygen sensor SBE43.

BIOLOGICAL INVESTIGATIONS

E. Abramova, A. Gukov

Lena Delta State Reserve, Tiksi, Russia

1. Introduction

The continental shelves of the Arctic Ocean and the surrounding marginal seas account for 70% of the Arctic Ocean surface and 25% of the Earth's shelf area. Recent studies indicate that these regions can be very productive. As large open areas of water in ice-covered regions, the shelf polynyas may be of considerable importance for the overall fixation, cycling, and storage of carbon in the Arctic marine ecosystem, since primary and secondary production may increase in ice-free regions (Smith, 1995). In the areas surrounding the polynyas, the interval between the break-up of the ice cover in mid-summer and the return of the polar light may be as short as two months. Hence, the season of development of herbivores should start earlier than in non-polynya areas of the Arctic (Prokopowicz and Fortier, 2002).

Global warming has resulted in an increase in seawater temperature and a reduction in the ice cover in the Arctic. This long-term development is complicated by the extensive inter-annual and regional variation that characterizes the Arctic shelves. Ecological changes naturally follow ecosystem alteration associated with global warming. Polynyas are particularly sensitive to the current changes in oceanic and atmospheric forcing. The effect of warming on polynyas affects all elements of the marine ecosystem, including benthic and pelagic processes as well as biochemical cycling and its rate. Therefore, polynya dynamics in the Arctic can markedly alter both the productivity and food web structure of high latitude marine environments (Arrigo and van Dijken, 2004). The understanding of biological processes in polynya regions may be critical to understanding and modelling the Arctic response to climate variability.

Currently, some basic knowledge regarding the food webs and their physical forcing exists for the Laptev Sea shelf and polynya region. However, further work in this region is urgently needed to investigate and analyze seasonal and inter-annual variability and changes in different components of the Laptev Sea shelf ecosystem in more detail.

The main aim of the biological investigations during the expedition was to collect data on the structure of food webs and productivity of marine ecosystems in the Laptev Sea, both under the fast ice cover and in the open waters of its polynya. This knowledge will help to analyze the response of Arctic marine ecosystems to the reduction of the Arctic sea ice cover due to global climate changes. Research tasks were:

- to study spatial and seasonal variations in the species composition, total abundance and biomass of phytoplankton, as well as primary production on the Laptev Sea shelf in dependence on the light and ice regimes, salinity and temperature conditions, water stratification and concentration of nutrients;
- to investigate the distribution pattern and variability of species composition, total abundance and biomass of pelagic and benthic fauna in relation to primary productivity, hydrological, hydrochemical and ice conditions.

2. Sampling activities during the expedition

During the POLYNYA 2008/TRANSDRIFT XIII expedition samples were collected for different biological analyses.

For measuring the chlorophyll *a* concentration and analyzing its distribution in the polynya

region we collected:

- 74 water samples (bathometer) from standard horizons at 14 stations. From each horizon 1 liter of water was collected. Water was then filtered through GFF filters, which were later frozen at -20°C in the freezing camera;
- 33 ice samples (upper, middle and lower 10 cm) from 11 ice cores. The ice was melted in the dark laboratory at a temperature not higher than 10°C. The meltwater was then filtered through GFF filters, which were later frozen at -20°C in the freezing camera.

For investigating the species composition of phytoplankton, its lateral and vertical distribution, and seasonal variations in water and ice we collected:

- 75 water samples (bathometer) from standard horizons at 15 stations. From each horizon 1 liter of water was collected. Water samples were fixed by 4% neutral formalin;
- 12 ice samples (upper, middle and lower 10 cm) from 4 ice cores. The ice was melted in the laboratory at a temperature not higher than 4°C. Water samples were fixed with 4% neutral formalin;
- 15 net-catch samples from the surface water layer (0-15 m). Net catches were performed through a hole in the ice by a hand net (opening diameter 20 cm, cone length 50 cm, meshsize 20 µm). The water samples were fixed with 4% neutral formalin.

For investigating pelagic fauna we collected 22 net zooplankton catches. Net catches were performed through a hole in the ice by a hand net (opening diameter 20 cm, cone length 50 cm, meshsize 100 µm). At each station net catches were made in the whole water column. Sampling was carried out from the fast ice edge as well as through a hole in the ice. Samples were fixed with 4% neutral formalin.

For investigating the composition and distribution of ice fauna we collected 48 ice samples. Ice cores were sawn into blocks: the lower 10 cm into 2-cm thick slices, and the remaining parts of the cores into 10-cm thick ones. Ice samples were melted in the laboratory at a temperature not higher than 10°C in excess of filtered seawater. The obtained samples were concentrated on a 20 µm sieve and fixed with 4% neutral formalin.

For investigating species composition of macrobenthos, bottom sediment samples were collected at 11 stations by a Van Veen grab sampler (coverage 250 cm²). Sampling was carried out from the fast ice edge as well as through a hole in the ice. In order to obtain a representative sample, at each station grab sampling was repeated 10 times. Benthos was fixed with 70% ethanol.

3. Preliminary results

As expected, the highest concentration of chlorophyll *a* was observed in the upper 5-m thick water layer (Fig. 29). The pigment in this layer is distributed unevenly with concentrations ranging from 0.05 to 1.37 mg/l at different stations. Chlorophyll *a* concentration increased in late April/early May due to algae bloom. Chlorophyll *a* concentration during this period was comparable to the values obtained in this region in September 2007 (BARKALAV 2007/TRANSDRIFT XII expedition).

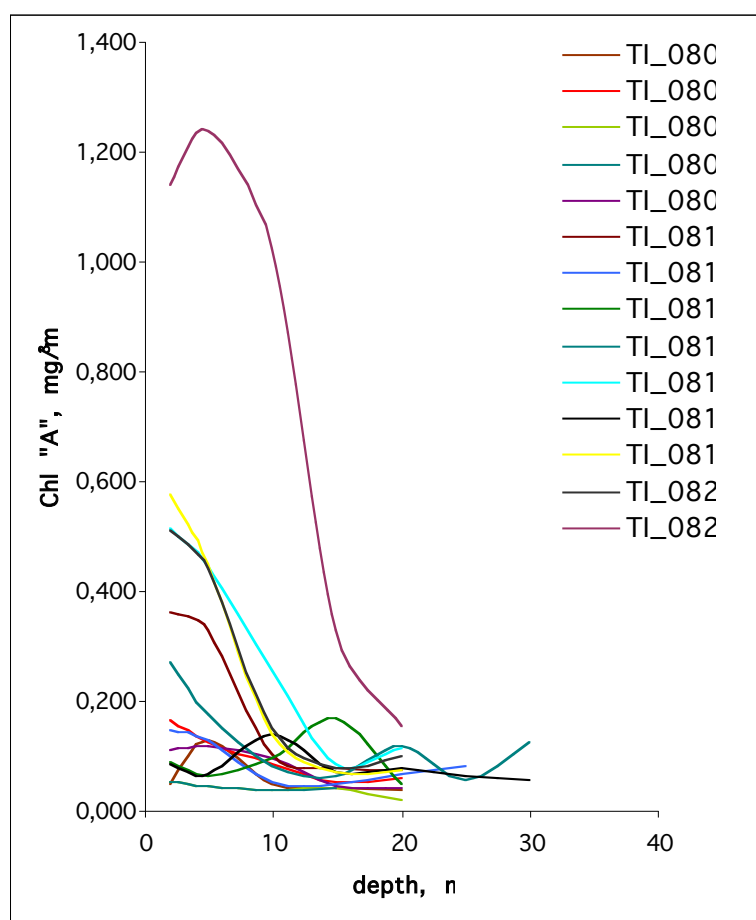


Fig. 29: Chlorophyll *a* concentration profiles at different stations of the POLYNYA 2008/TRANSDRIFT XIII expedition.

To measure the chlorophyll *a* concentration in the water column, we also used the sensor which was attached to the SBE19 probe. Analysis of sensor record with measured concentrations showed the correlation coefficient between the two curves to be rather high. However, sensor data are on average 3-4 times higher than the values obtained by filter processing (Fig. 30).

Ice samples were found to be enriched in chlorophyll *a* in comparison with water samples. Its concentration in the basal 10 cm of ice at 10 stations varied between 3.0 and 19.7 mg/l. The highest chlorophyll *a* concentration in the ice reached 97.4 mg/l at station 13.

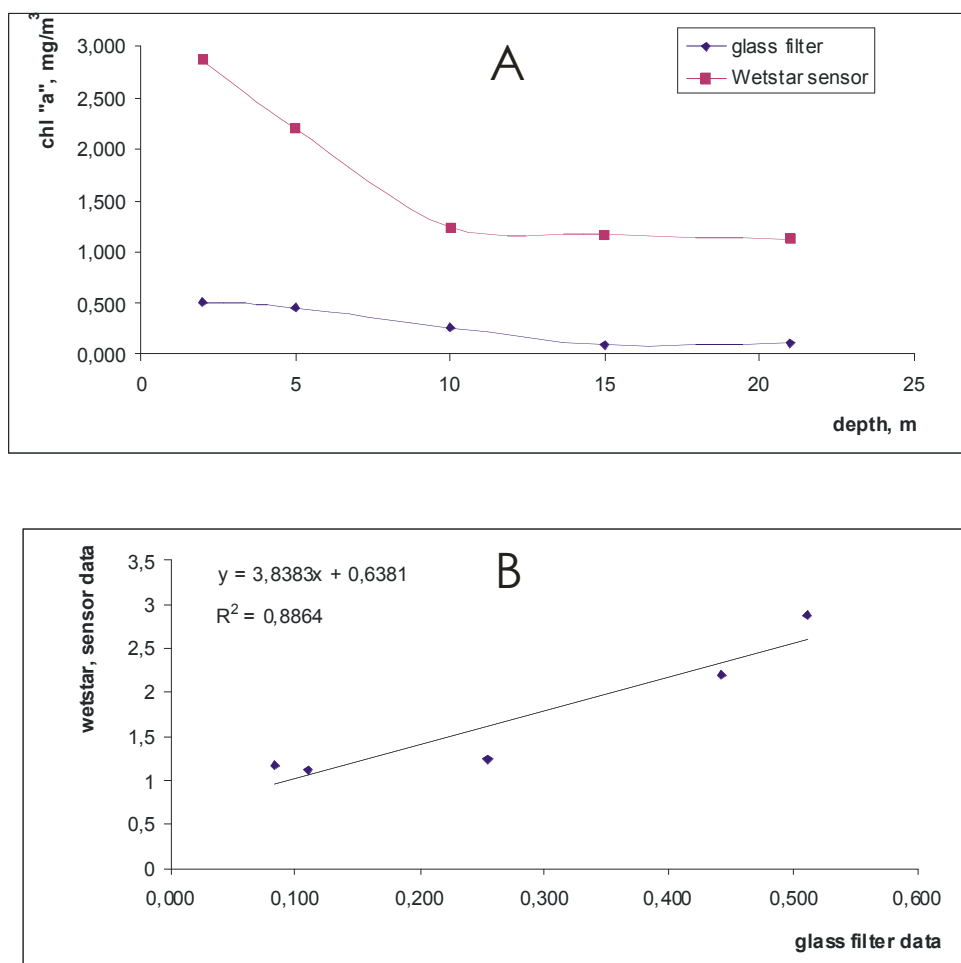


Fig. 30: Chlorophyll *a* profiles recorded by sensor and measured by filter processing (A); correlation between sensor and measured data (B).

Zooplankton was found to be represented by 20 taxa, 10 of which being different Copepoda. Two species were the most abundant among adult Copepoda: the cosmopolitan marine euryhaline species *Oithona similis* (Fig. 31A) and the euryhaline brackish-water species *Acartia longiremis* (Fig. 31B). Copepod nauplii were the most abundant organisms in the planktic fauna, while Polychaeta predominated among other groups.

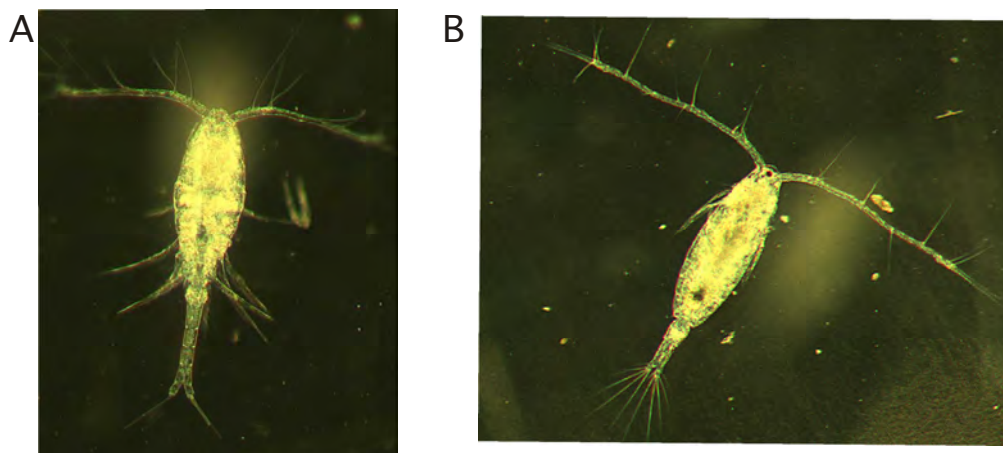


Fig. 31: Zooplankton species found to be the most abundant in the southeastern Laptev Sea during the POLYNYA 2008/TRANSDRIFT XIII expedition. A – *Oithona similis*, B – *Acartia longiremis*.

The ice fauna was found to be largely represented by Nematoda, Harpacticoida, Rotatoria and Protozoa. Single Ostracoda were found in some samples. The highest abundance of organisms was observed in the basal ice layers.

Zoobenthos samples were collected at 11 stations. The samples are dominated by five major faunal groups with brittle stars, bivalves and polychaets being the most abundant. Gastropods and crustaceans are less abundant, but also numerous. The most taxonomically diverse bottom biocoenoses occur on muddy and sandy-muddy grounds. The biocoenoses are dominated by the bivalve species *Leionucula tenuis* and *Tridonta borealis* together with the brittle star species *Ophiecten sericeum*.

4. Preliminary conclusions

It is known that in the Arctic seas algae occurring on the lower ice surface are the main food source for the planktic fauna during wintertime. Our data on the chlorophyll *a* concentration also show that algae are most abundant at the lower ice surface. The observed decrease of the ice cover extent due to climate changes might cause re-distribution of primary productivity and alteration of the Arctic food webs and ecosystems.

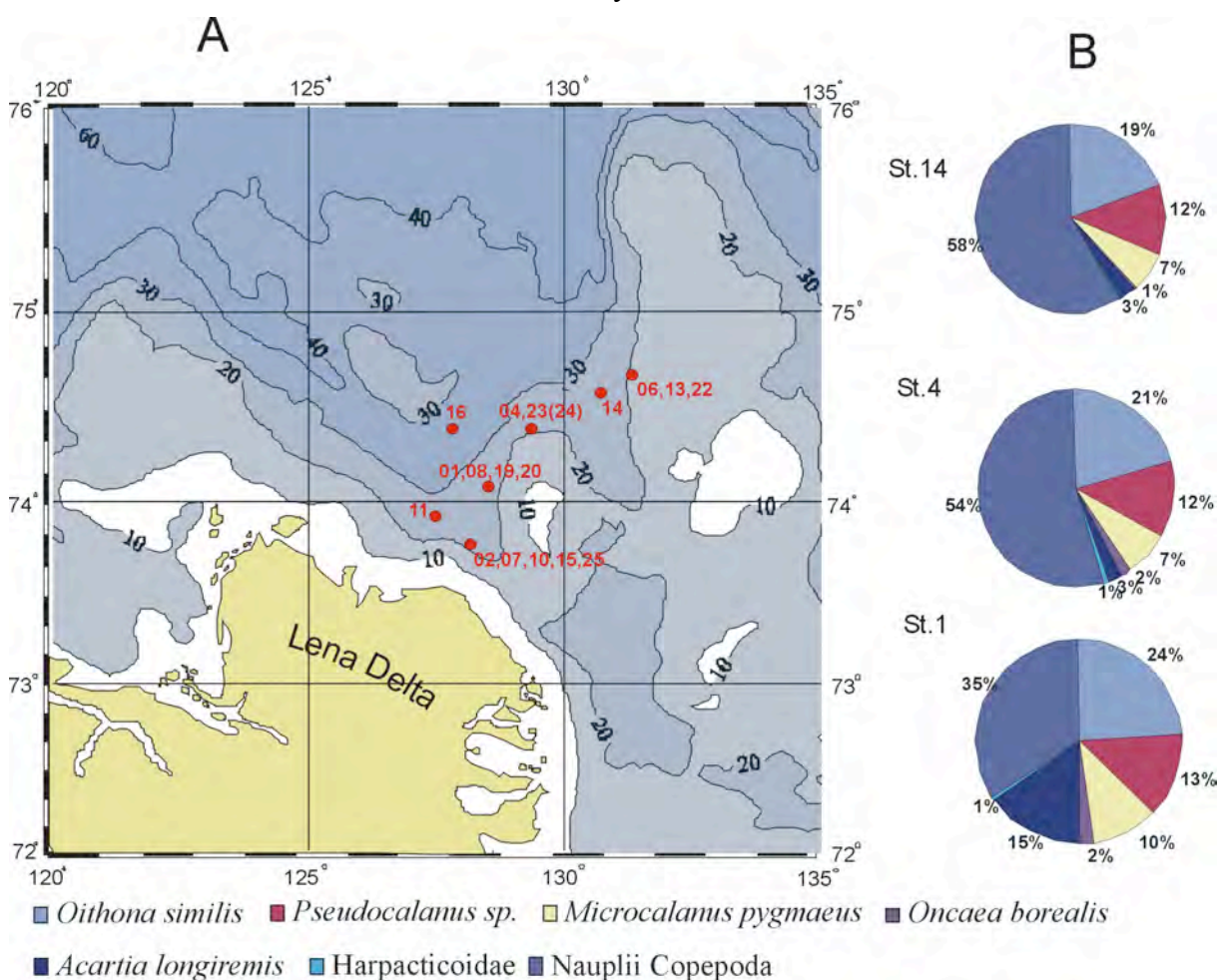


Fig. 32: A – stations of the POLYNYA 2008/TRANSDRIFT XIII expedition (April-May 2008); B – relative abundance of different Copepoda species at stations 1, 4 and 14.

Evident changes are already observed in the species composition, dominant species and relative representation of planktic fauna. According to the average multiannual data (1993-2004) during summer zooplankton in the study area was dominated by an *Oithona similis* –

Pseudocalanus sp. – *Drepanopus bungei* assemblage. In April 1999 (TRANSDRIFT VI expedition) *D. bungei* represented 80% of the total zooplankton abundance. During this year's expedition only rare specimens of *D. bungei* were found at several stations (Fig. 32). The relative abundance of *Oithona similis* and *Microcalanus pygmaeus* sharply increased (up to 60%) (Fig. 32). These species are typical representatives of the Laptev Sea continental slope association. Thus, the observed changes could be related to the growing influence of open-sea waters on the inner shelf regions. Most likely, the observed increase in abundance of *Acartia longiremis* is due to the same reasons as this species is considered to be an indicator of Atlantic-derived waters (Hirche et al., 2006).

PRELIMINARY SCIENTIFIC AND PRACTICAL RESULTS OF THE POLYNYA 2008/TRANSDRIFT XIII EXPEDITION

L. Timokhov¹, H. Kassens², A. Novikhin¹, S. Kirillov¹

¹State Research Center – Arctic and Antarctic Research Institute, St. Petersburg, Russia

²IFM-GEOMAR, Leibniz Institute of Marine Sciences, Kiel, Germany

The investigations carried out during the POLYNYA 2008/TRANSDRIFT XIII expedition contributed to the implementation of the IPY program. The expedition enlarged the oceanographic database of the Russian Hydrometeorological Survey and the AARI. Complex data about the Arctic environment during wintertime were obtained.

Some oceanographic stations were deployed in the same positions as the bottom stations of the summer BARKALAV 2007/ TRANSDRIFT XII expedition. Other stations were deployed within the area of the oceanographic polygon made during that expedition. This allows us to record seasonal variability of water mass properties and to analyze manifestations of the physical, hydrochemical and hydrobiological processes in the study area.

The oceanographic measurements revealed the presence of relatively warm Atlantic-derived waters in the bottom water layer of the southern Laptev Sea shelf. The reduced concentration of dissolved oxygen also recorded in the bottom water layer is comparable to the climate minimum values.

At the same time, at some stations the vertical thermohaline and hydrochemical profiles did not show any evident changes.

Our new results together with the data obtained during previous expeditions provide important information for the improvement and validation of the models used in climate research describing interactions between atmospheric circulation, ocean currents and sea ice drift.

During the expedition water samples were collected at 17 oceanographic stations. Dissolved oxygen concentration was determined in 39 samples. Eighty-four samples for nutrients (phosphates, silicates and nitrate-nitrites) will be measured in the OSL.

The concentration of dissolved oxygen varied from 5.67 ml/l (station 14; bottom water layer) to 8.96 ml/l (station 9; 5-m water depth). At the northern stations (14 and 19) the bottom water layers were oxygen-depleted (less than 6 ml/l). These data are in agreement with the existing idea about the distribution pattern of dissolved oxygen and nutrients in the study area.

Water samples were also taken for chlorophyll *a* measurements and investigations of phyto and zooplankton composition. Ice was sampled for analysis of the composition and abundance of ice fauna, and bottom sediments were collected for benthos analysis.

Currently the data are being prepared for the AARI database and the state environmental database of the Russian Federation (Obninsk). Oceanographic, meteorological and ice observational data are being prepared for the international exchange according to existing rules and the permission for marine scientific investigations.

The data obtained during the expedition give important information for:

- continuation of the complex monitoring of the Laptev Sea polynya and water mass changes in the adjacent regions;
- assessment of heat, salt and momentum fluxes in different oceanic water layers from the surface to the sea floor;
- estimation of the amount of suspended and dissolved organic and inorganic matter;

- determination of the components of inorganic nitrogen and phosphorus cycles in the study area.

Cooperation between the AARI, IFM-GEOMAR and AWI allowed for obtaining original observational data and enlarging the oceanographic database, which is the basis for future scientific research.

REFERENCES

- Abramova, E. and Tuschling, K. (2005) A 12-year study of the seasonal and interannual dynamics of mesozooplankton in the Laptev Sea: significance of salinity regime and life cycle patterns. *Global and Planetary Change*, 48(1-3): pp. 141-164.
- ACIA (2004) *Impacts of a Warming Arctic: Arctic Climate Impact Assessment*. Cambridge University Press, 139 pp.
- Arrigo, K.R. and van Dijken, G.L. (2004) Annual cycles of sea ice and phytoplankton in Cape Bathurst polynya, southeastern Beaufort Sea, Canadian Arctic. *Geophysical Research Letters*, 31(1-4), L08304, doi:10.1029/2003GL018978.
- Dmitrenko, I.A., Tyshko, K.P., Hoelemann, J.A., Eicken, H. and Kassens, H. (2002) Water circulation and crystal structure of sea ice in the marginal area of the Laptev Sea flaw polynya. *Meteorologiya i gidrologiya*, 8: pp. 67-76 (in Russian).
- Dmitrenko, I., Kirillov, S., Eicken, H. and Markova, N. (2005a) Wind-driven summer surface hydrography of the eastern Siberian shelf. *Geophysical Research Letters*, 32, L14613, doi:10.1029/2005GL023022.
- Dmitrenko, I., Tyshko, K., Kirillov, S., Hoelemann, J., Eicken, H. and Kassens, H. (2005b) Impact of flaw polynyas on the hydrography of the Laptev Sea. *Global and Planetary Change*, 48, pp. 9-27, doi:10.1016/j.gloplacha.2004.12.016.
- Dmitrenko, I.A., Kirillov, S.A. and Tremblay, L.B. (2007) The long-term and interannual variability of summer fresh water storage over the eastern Siberian Shelf. Implication for climatic change. *Journal of Geophysical Research*, doi:10.1029/2007JC004304.
- Frolov, I.E. and Gavrilov, V.P. (eds.) (1997) *Sea Ice. Collection and Analysis of Observational Data, Physical Properties, and Forecast of Ice Conditions (Reference Materials)*. St. Petersburg: Gidrometeoizdat, 402 pp. (in Russian).
- Haas, C. (2004) Late-summer sea ice thickness variability in the Arctic Transpolar Drift 1991-2001 derived from ground-based electromagnetic sounding. *Geophysical Research Letters*, 31, L09402, doi:10.1029/2003GL019394.
- Hirche, H.J., Kosobokova, K.N., Gaye-Haake, B., Harms, I., Meon, B. and Nothig, E.-M. (2006) Structure and function of contemporary food webs on Arctic shelves: A panarctic comparison. The pelagic system of the Kara Sea - Communities and components of carbon flow. *Progress in Oceanography*, 71: pp. 288-313.
- Johannessen, O.M., Miles, M. and Bjorgo, E. (1995) The Arctic's shrinking sea ice. *Nature*, 376: pp. 126-127.
- Kirillov, S., Makhotin, M. and Dmitrenko, I. (in press) Thermohaline structure of Siberian shelf waters: climatic variability and key sources. In: *The System of the Laptev Sea and Adjacent Arctic Seas: Modern Environment and Paleoclimate* (in Russian).
- Lyalyagin, N.A. and Tyshko, K.P. (2002) Influence of sea ice crystal structure on the formation and variability of the vertical salinity distribution in one-year ice. *Meteorologiya i gidrologiya*, 2: pp. 64-71. (in Russian).
- Maslanik, J.A., Serreze, M.C. and Barry, R.G. (1996) Recent decreases in Arctic summer ice cover and linkages to atmospheric circulation anomalies. *Geophysical Research Letters*, 23: pp. 1677-1680.
- Morales Maqueda, M.A. and Willmott, A.J. (2000) A two-dimensional time-dependent model of a latent heat coastal polynya. *Journal of Physical Oceanography*, 30: pp. 1281-1304.
- Polyakov, I.V., Alexeev, G.V., Timokhov, L.A., Bhatt, U.S., Colony, R.L., Simmons, H.L., Walsh, D., Walsh, J.E. and Zakharov, V.F. (2004) Variability of the intermediate Atlantic Water of the Arctic Ocean over the last 100 years. *Journal of climate*, 17(23): pp. 4485-4497.
- Polyakov, I., Beszczynska, A., Carmack, E., Dmitrenko, I., Fahrbach, E., Frolov, I., Gerdes, R., Hansen, E., Holfort, J., Ivanov, V., Johnson, M., Karcher, M., Kauker, F., Morison, J., Orvik, K., Schauer, U., Simmons, H., Skagseth, O., Sokolov, V., Steele, M., Timokhov, L., Walsh, D. and Walsh, J. (2005) One more step toward a warmer Arctic. *Geophysical Research Letters*, 32, doi:10.1029/2005GL023740.
- Prokopowicz, A. and Fortier, L. (2002) Population structure of three dominant *Calanus* species in North Water Polynya, Baffin Bay. *Polish Polar Research*, 23(3-4): pp. 241-252.
- Rothrock, D.A., Yu, Y. and Maykut, G.A. (1999) Thinning of the Arctic sea-ice cover. *Geophysical Research Letters*, 26: pp. 3469-3472.

- Schauer, U., Rudels, B., Jones, E.P., Anderson, L.G., Muench, R.D., Björk, G., Swift, J.H., Ivanov, V. and Larsson, A.-M. (2002) Confluence and redistribution of Atlantic water in the Nansen, Amundsen and Makarov basins. *Annales Geophysicae*, 20: pp. 257-273.
- Smagin, V., Pivovarov, S., Morozova, O., Nitishinskii, M. and Novikhin, A. (2003) Nutrient budgets in the coastal areas, estuaries, and estuarine zones in the Siberian Arctic seas. *AARI Proceedings*, pp. 16-17 (in Russian).
- Smagin, V. and Novikhin, A. (2007) Influence of the Atlantic waters inflow on the nutrients vertical distribution in the Arctic Ocean. *Problemy Arktiki i Antarktiki (Arctic and Antarctic Problems)*, 75: pp. 43-49 (in Russian).
- Smith, W.O. (1995) Primary productivity and new production in the Northeast Water (Greenland) Polynya during summer 1992. *Journal of Geophysical Research*, 100: pp. 4357-4370.
- Tyshko, K.P. (2007) Structural classification of dynamomethamorphic modifications of one-year sea ice. *Meteorologiya i gidrologiya*, 8: pp. 69-76 (in Russian).
- Tyshko, K.P. and Kovalev, S.M. (2006) The role of water-shuga layers in the growth of one-year ice and consolidation of pressure ridges. *Meteorologiya i gidrologiya*, 8: pp. 72-82 (in Russian).

APPENDIX

- List of participants
- Station map
- List of stations

TRANSDRIFT XIII - PARTICIPANTS

Name	Institute	E-Mail
Abramova, Ekaterina	Lena Delta Reserve / OSL	Abramova-Katya@mail.ru
Dmitrenko, Igor	IFM-GEOMAR	idimitrenko@ifm-geomar.de
Eden, Ralf	Generalkonsulat der BRD in St. Petersburg	ralf.eden@diplo.de
Egikov, Sergey	Lena Delta Reserve	lena_delta@rumbler.ru
Esipenko, Sergey	Lena Delta Reserve	lena_delta@rumbler.ru
Ernsdorf, Thomas	University of Trier	erns6b02@uni-trier.de
Gukov, Alexander	Lena Delta Reserve	lena_delta@rumbler.ru
Helbig, Alfred	University of Trier	helbig@uni-trier.de
Hölemann, Jens	AWI	jens.hoelemann@awi.de
Isenberg, Marc-André	IFM-GEOMAR	dwj-euro@web.de
Kassens, Heidemarie	IFM-GEOMAR	hkassens@ifm-geomar.de
Kirillov, Sergey	AARI / OSL	dia@aari.nw.ru
Klagge, Torben	IFM-GEOMAR	tklagge@ifm-geomar.de
Krumpen, Thomas	AWI	tkrumpen@awi.de
Makhotin, Mikhail	AARI / OSL	m-makhotin@mail.ru
Novikhin, Andrey	AARI / OSL	asghard@rambler.ru
Rabenstein, Lasse	AWI	lasse.rabenstein@awi.de
Taldenkova, Ekaterina	Moscow State University	etaldenkova@mail.ru
Tyshko, Konstantin Pavlovich	AARI	tyshko@aari.nw.ru
Vizitov, Viktor Grigorievich	AARI	vizitov@aari.nw.ru
Vorobyev, Ivan	Lena Delta Reserve	lena_delta@rumbler.ru

IFM-GEOMAR, Wischhofstr. 1-3, Gebäude Ostufer, 24148 Kiel, Germany

AWI, Bussestr. 24, 27570 Bremerhaven, Germany

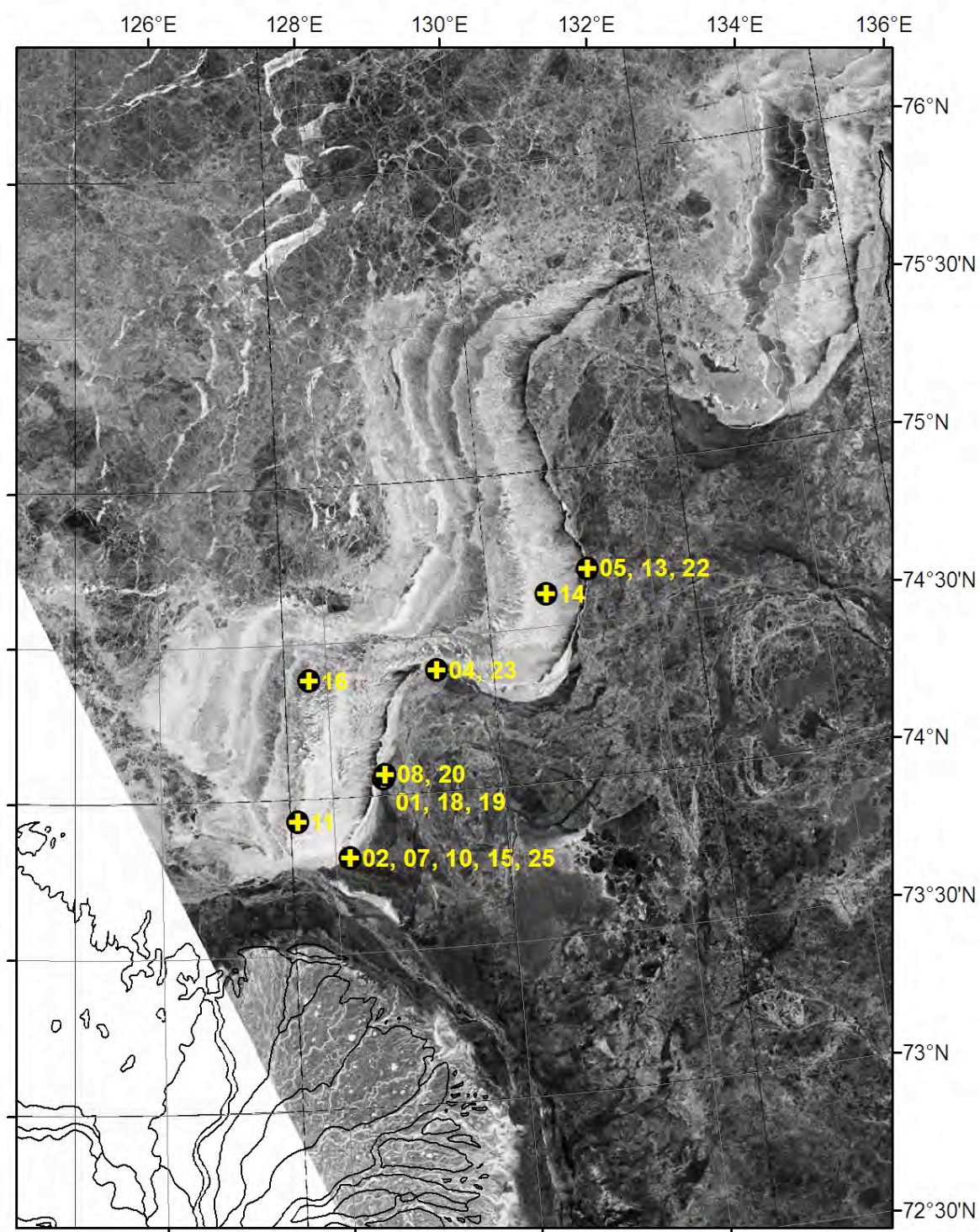
University of Trier, Behringstr. 21, (Campus II), 54286 Trier, Germany

Generalkonsulat der BRD in St. Petersburg, Ul. Furshtatskaja 39, 191123 St. Petersburg, Russia


AARI / OSL, Ul. Beringa 38, 199397 St. Petersburg, Russia


Lena Delta Reserve, Akademika Fedorova Ul. 28, 678400 Tiksi, Russia

Moscow State University, GSP-2, Leninskie Gory, 119992 Moscow, Russia



ASAR WSM Imagery,
Date: 20080501 12:01 UTC
Projection: Polar Stereo. WGS-84

 TDXIII Stations

0 25 50 100 Kilometers


TRANSDRIFT XIII - Station list

Station #	Date	Time (Tiksi)	Latitude (° N)	Longitude (° E)	Depth (m)	Activity	Notes
TI 08 01	10.4.2008	13:35	74°03.983	128°37.868	24	begin of station	fast ice 67 cm; new ice 20 cm Position 74°04.054; 128°37.537
-1		15:15				water sampling for oxygen, chlorophyll, nutrients, phytoplankton	1, 5, 10, 15, 20 m
-2		16:07				CTD with sensors for turbidity, oxygen, chlorophyll A	
-3		16:15				net	18 cm diameter; 100 µm
		16:20				net	18 cm diameter; 20 µm
		16:30				ice core (9 cm diameter): ice biology	2 cores
-4		16:40				deployment mooring (2 CTD, 1 ADCP 300 kHz)	microcats 3049 at 3 m, 4975 at 20 m; ADCP 296 at 2.5 m
-5		14:00				ice physics	2 ice cores, temperature, salinity and textural analysis
		18:00				end of station	
TI 08 02	11.4.2008	13:00	73°48.319	128°09.753	21	begin of station	fast ice 57 cm
-1		14:00				CTD with sensors for turbidity, oxygen, chlorophyll A	
-2		14:20				water sampling for oxygen, chlorophyll, nutrients, phytoplankton	1, 5, 10, 15, 20 m
-3		15:05				net	18 cm diameter; 100 µm
						net	18 cm diameter; 20 µm
-4		16:05	73°48.334	128°09.673		ice core (9 cm diameter): ice biology	2 cores
-5		15:50				deployment mooring (2 CTD, 1 ADCP 300 kHz)	microcats 2308 at 3 m, 4976 at 18 m; ADCP 567 at 2 m
-6		17:15	73°48.261	128°09.891		CTD	1 cast
-7		17:23	73°48.203	128°10.020		CTD	1 cast
-8		17:31	73°48.147	128°10.121		CTD	1 cast
-9		17:39	73°48.088	128°10.229		CTD	1 cast
-10						ice physics	2 ice cores, temperature, salinity, and textural analysis
-11						Meteorological station No 1 deployed	
-12						ice core for oxygen	57 cm, cut into slices of 10 cm
		17:55				end of station	
TI 08 03	10.4.2008	15:55	73°46.73	128°23.90		start of EM bird profile / ice observation	WP 74°15'00"N, 127°56'00"E, 210 km
	10.4.2008	17:20	73°43.88	127°16.44		end of EM bird profile / ice observation	no HEM bird data
TI 08 04	12.4.2008	11:59	74°23.355	129°19.170	19,8 m	begin of station	Wind E; -17°C; fast ice 1.45 m
-1		12:40				ice physics; 1 ice core	fall fast ice 1.45 m
-2		12:15				Meteorological station No 2 deployed	74°23'23,4"
-3		12:40				Biology benthos sampling (snapper)	distance to open water 300 m
-4		12:55				CTD with sensors for turbidity, oxygen, chlorophyll A	
-5		13:10				ice core (9 cm diameter): ice biology - fauna	3 cores
-6		13:15				water sampling for oxygen, chlorophyll, nutrients, phytoplankton	2m, 5m, 10m, 15m, 19m
						net	18 cm diameter; 100 µm
						net	18 cm diameter; 20 µm
-7		13:30				deployment mooring (2 CTD, 1 ADCP 300 kHz)	ADCP 2m, CTD 10m, 17m
		16:00				end of station	

TRANSDRIFT XIII - Station list

Station #	Date	Time (Tiksi)	Latitude (° N)	Longitude (° E)	Depth (m)	Activity	Notes
TI 08 05	14.04.2008	13:42	74°40.352	131°14.674	18	begin of station	fast ice 62 cm; 7 cm snow
-1		14:15				CTD with sensors for turbidity, oxygen, chlorophyll A	
-2		14:30				water sampling for oxygen, chlorophyll, nutrients, phytoplankton	2, 5, 10, 17 m
-3		15:10				net	18 cm diameter; 100 µm
						net	18 cm diameter; 20 µm
						ice core (9 cm diameter): ice biology	3 cores
-4		15:30				deployment mooring (2 CTD, 1 ADCP 300 kHz)	microcats 5388 at 3 m, 1604 at 17 m; ADCP 7944 at 2 m
-5		14:05	74°40.365	131°14.745		Meteorological station No 3 installation	
-6						ice physics	2 ice cores, temperature, salinity and textural analysis
-7		13:50				fishing at the ice edge	
-8		14:30				Biology benthos sampling (snapper)	
		16:32				end of station	
TI 08 06	14.04.2008	16:00	74°40.319	131°14.674		start of EM bird profile	
						end of EM bird profile	
TI 08 07	14.04.2008	17:21	73°48.319	128°09.753		begin of station	
-1		18:10				CTD	2 casts
-2		17:30				Biology benthos sampling (8 snapper)	
		18:18				end of station	
TI 08 08	16.4.2008	11:46	74°03.325	128°36.465	22.4 m	begin of station	30 cm new ice
-1		12:35				CTD with sensors for turbidity, oxygen, chlorophyll A	2 casts
-2		12:50				water sampling for oxygen, chlorophyll, nutrients, phytoplankton	2, 5, 10, 15, 20
-3		13:10				net	18 cm diameter; 100 µm
						net	18 cm diameter; 20 µm
						ice core (9 cm diameter): ice biology	2 cores
-4		14:40	74°03.312	128°36.451		deployment mooring (1 CTD, 1 ADCP 300 kHz)	microcats 5387 at 17 m, ADCP 3845 at 3 m
-5		15:44	74°03.346	128°36.309			1 cast
-6		15:50	74°03.364	128°36.206			1 cast
-7		15:55	74°03.381	128°36.114			1 cast
-8		16:02	74°03.411	128°35.977			1 cast
TI 08 09	16.04.2008	13:46	74°40.319	131°14.674		start of EM bird profile	WP 1: 74°03, 128°38; WP 2: 74°26, 125°00;
		16:20				end of EM bird profile	WP 3: 74°39, 125°43

TRANSDRIFT XIII - Station list

Station #	Date	Time (Tiksi)	Latitude (° N)	Longitude (° E)	Depth (m)	Activity	Notes
TI 08 10	19.04.2008	12:00	73°48.313	128°09.725	21 m		Station 2
-1		12:07	73°48.313	128°09.725		CTD with sensors for turbidity, oxygen, chlorophyll A	fast ice 68
-2		12:20	73°48.313	128°09.725		water sampling for oxygen, chlorophyll, nutrients, phytoplankton	2, 5, 10, 15 m
-3		12:45				ice physics; 2 ice core	65 cm fast ice, temperature, salinity
-4		13:00				net	40 cm diameter; 55 µm
-5		13:15	73°48.334	128°09.671		Mini box core	new ice
-6		13:40				net	18 cm diameter; 100 µm
-7		13:45				net	18 cm diameter; 20 µm
-8		12:28	73°48.334	128°09.671		CTD	31 cm new ice
-9		12:36	73°48.365	128°09.562		CTD	26 cm new ice
-10		12:42	73°48.390	128°09.424		CTD	28 cm new ice
-11		12:51	73°48.417	128°09.292		CTD	28 cm new ice
-12		12:59	73°48.456	128°09.183		CTD	30 cm new ice
-13		13:05	73°48.404	128°09.099		CTD	26 cm new ice
-14		13:12	73°48.549	128°09.013		CTD	25 cm new ice
-15		13:42	73°48.086	128°10.236		CTD	68 cm fast ice
-16		13:49	73°48.146	128°10.124		CTD	68 cm fast ice
-17		13:56	73°48.203	128°10.019		CTD	68 cm fast ice
-18		14:05	73°48.265	128°09.890		CTD	60 cm fast ice
-19		14:10				ice core (9 cm diameter): ice biology and fauna	3 cores
-20		12:05				Biology benthos sampling (8 snapper)	
		14:18				end of station	
TI 08 11	19.04.2008	14:42	73°55.707	127°34.874	24.7 m	begin of station	drifting fast ice 110 cm
-1		15:13	73°55.707	127°34.874		CTD with sensors for turbidity, oxygen, chlorophyll A	new ice 32 cm
-2		15:45				water sampling for oxygen, chlorophyll, nutrients, phytoplankton	2, 5, 10, 15, 20 ,23 m
-3		16:10				net	18 cm diameter; 100 µm
						net	18 cm diameter; 20 µm
-4						ice physics	2 ice cores, temperature, salinity, textural analysis
-5		15:20				Biology benthos sampling (8 snapper)	
-6		16:05	73°55.657	127°35.051		CTD	30 cm new ice
-7		16:12	73°55.609	127°35.231		CTD	30 cm new ice
-8		16:20	73°55.556	127°35.414		CTD	31 cm new ice
-9		16:26	73°55.511	127°35.637		CTD	31 cm new ice
-10						ice core (9 cm diameter): ice biology	2 cores
		16:52				end of station	
TI 08 12	19.04.2008	13:46	74°40.319	131°14.674		start of EM bird profile	WP 1: 74°03, 128°38; WP 2: 74°26, 125°00;
	19.04.2008	16:20				end of EM bird profile	WP 3: 74°39, 125°43

TRANSDRIFT XIII - Station list

Station #	Date	Time (Tiksi)	Latitude (° N)	Longitude (° E)	Depth (m)	Activity	Notes
TI 08 13	21.04.2008	13:04	74°40.361	131°14.672	18.8 m	begin of station	Station TI0805; fast ice edge 39 cm
-1		13:29	74°40.361	131°14.672		CTD with sensors for turbidity, oxygen, chlorophyll A	
-2		13:38				water sampling for oxygen, chlorophyll, nutrients, phytoplankton	2, 5, 10, 15, 18 cm
-3		14:10				net	18 cm diameter; 100 μ m
						net	18 cm diameter; 20 μ m
						ice core (9 cm diameter): ice biology	2 cores
-4		13:57	74°40.352	131°14.360		CTD	40 cm new ice
-5		14:05	74°40.359	131°14.079		CTD	37 cm new ice
-6		14:12	74°40.383	131°13.831		CTD	32 cm new ice
-7		14:21	74°40.405	131°13.574		CTD	31 cm new ice
-8		14:46	74°40.354	131°14.686		CTD	140 cm fast ice
-9		14:57	74°40.357	131°14.825		CTD	145 cm fast ice
-10						ice physics	125 cm fast ice; salinity and temperature
-11						ice core for oxygen	72 cm
						Biology benthos sampling (8 snapper)	
		15:01				end of station	
TI 08 14	21.04.2008	15:23	74°36.218	130°42.877	28.4 m	begin of station	drifting fast ice 125 cm
-1		15:38	74°36.218	130°42.877		CTD with sensors for turbidity, oxygen, chlorophyll A	32 cm new ice
-2		15:56				water sampling for oxygen, chlorophyll, nutrients, phytoplankton	2, 5, 10, 15,20,25, 28 m
-3		16:20				net	18 cm diameter; 100 μ m
						net	18 cm diameter; 20 μ m
						ice core (9 cm diameter): ice biology	2 cores
-4		16:16	74°36.092	130°43.808		CTD	35 cm new ice
-5		16:26	74°36.121	130°43.556		CTD	30 cm new ice
-6		16:37	74°36.150	130°43.321			32 cm new ice
-7		16:44	74°36.180	130°43.108			32 cm new ice
-8						ice physics	2 ice cores, temperature, salinity, textural analysis
-9						ice core for oxygen	65 cm
						Biology benthos sampling (8 snapper)	
						ice core (9 cm diameter): ice biology	2 cores
		17:30				end of station	

TRANSDRIFT XIII - Station list

Station #	Date	Time (Tiksi)	Latitude (° N)	Longitude (° E)	Depth (m)	Activity	Notes
TI 08 15	24.04.2008	12:37	73°48.318	128°09.730	20.7 m		Station 2
-1		13:03				CTD with sensors for turbidity, oxygen, chlorophyll A	
-2		13:12				water sampling for oxygen, chlorophyll, nutrients, phytoplankton	2, 5, 10, 15, 21
-3		13:30				net	18 cm diameter; 100 µm
						net	18 cm diameter; 20 µm
-4		13:18	73°48.335	128°09.679		CTD	36 cm new ice
-5		13:24	73°48.366	128°09.560		CTD	35 cm new ice
-6		13:34	73°48.548	128°09.005		CTD	32 cm new ice
-7		13:40	73°48.504	128°09.105		CTD	35 cm new ice
-8		13:47	73°48.457	128°09.183		CTD	38 cm new ice
-9		13:52	73°48.417	128°09.289		CTD	39 cm new ice
-10		14:03	73°48.265	128°09.885		CTD	60 cm fast ice
-11		14:10	73°48.201	128°10.017		CTD	69 cm fast ice
-12		14:16	73°48.146	128°10.129		CTD	65 cm fast ice
-13		14:20	73°48.091	128°10.223		CTD	89 cm fast ice
						Biology benthos sampling (8 snapper)	
						ice core (9 cm diameter): ice biology	2 cores
		14:56				end of station	
TI 08 16	24.04.2008	15:38	74°22.835	127°47.146	33.8 m		drifting ice 168 cm
-1		16:05				CTD with sensors for turbidity, oxygen, chlorophyll A	
-2		16:20	74°22.6	127°47.013		CTD with sensors for turbidity, oxygen, chlorophyll A	
-3		16:25				water sampling	2,5,10,15,20,25,30
-4		17:00				net	18 cm diameter; 100 µm
						net	18 cm diameter; 20 µm
-5		17:19	74°22.319	127°46.849		GPS position 2	strong drift
						Biology benthos sampling (8 snapper)	
-6		17:37				ice core (9 cm diameter): ice biology	2 cores
						end of station	
TI 08 17	24.04.2008					start of EM bird profile	WP aus der Planung
						end of EM bird profile	
TI 08 18	24.04.2008		74°03.325	128°36.465			
-1						Meteorologie	
TI 08 19	28.04.2008	13:05	74°03.317	128°36.435		start	40 cm new ice, polar bear !
-1		13:35				water sampling	2, 5,10, 15, 20
-2		13:43				CTD with sensors for turbidity, oxygen, chlorophyll A	
-3		13:05 - 13:30				Mooring recovery of TI0808	
-4		14:26				net	
		14:42				end of station	
TI 08 20	28.04.2008	15:00	74°03.985	128°37.846	22.9 m	start	78 cm ice thickness
-1		15:26				water sampling for oxygen, chlorophyll, nutrients, phytoplankton	2, 5, 10, 15, 23
						net	18 cm diameter; 100 µm
						net	18 cm diameter; 20 µm
-2		15:36				CTD with sensors for turbidity, oxygen, chlorophyll A	
-3		13:05 - 17:02				Mooring recovery of TI0801	
-4		17:05				Mini box core	
						ice core (9 cm diameter): ice biology	2 cores
		17:07				end of station	

TRANSDRIFT XIII - Station list

Station #	Date	Time (Tiksi)	Latitude (° N)	Longitude (° E)	Depth (m)	Activity	Notes
TI 08 21		12:45				start of EM-Bird profile	
		14:10				end of EM-Bird profile	
TI 08 22	29.4.2008	11:12	74°40.352	131°14.674	18.6 m		74 cm ice thickness
-1		11:34				water sampling for oxygen, chlorophyll, nutrients, phytoplankton	2, 5, 10, 15, 18
-2		11:41				CTD with sensors for turbidity, oxygen, chlorophyll A	
-3		12:21				net	18 cm diameter; 100 µm
						net	18 cm diameter; 20 µm
-4		11:15 - 12:30				Mooring recovery of TI0805	
-5		11:25 - 12:40				Meteorological station recovered	
						ice core (9 cm diameter): ice biology	2 cores
		12:33				end of station	
TI 08 23	29.4.2008	13:00	74°23.406	129°19.182	20 m	start	151 cm fast ice
-1		13:25				CTD with sensors for turbidity, oxygen, chlorophyll A	
-2		13:35				water sampling for oxygen, chlorophyll, nutrients, phytoplankton	2, 5, 10, 15, 19
						net	18 cm diameter; 100 µm
						net	18 cm diameter; 20 µm
-3		13:00 - 14:45				Mooring recovery of TI0804	
-4		14:10 - 15:05				Meteorological station recovered	damage by polar bear
						ice core (9 cm diameter): ice biology	3 cores
		15:04				end of station	
TI 08 25	4.5.2008	11:36	73°48.321	128°09.721	21,3 m	start	87 cm ice thickness
		11:57				CTD with sensors for turbidity, oxygen, chlorophyll A	
		12:04				water sampling for oxygen, chlorophyll, nutrients, phytoplankton	2, 5, 10, 15, 20 m
		11:40 - 12:25				Mooring recovery of TI0805	80 cm ice thickness
		14:52:00 - 15:52:00	73°50.321	128°06.755		NEMO float deployment	fast ice edge 8 cm ice thickness; navigation onboard helicopter
		12:42	73°48.338	128°09.672		CTD	47 cm
		12:50	73°48.369	128°09.556		CTD	40 cm
		12:57	73°48.399	128°09.438		CTD	38 cm
		13:03	73°48.429	128°09.327		CTD	42 cm
		13:09	73°48.462	128°09.207		CTD	42 cm
		13:14	73°48.497	128°09.114		CTD	36 cm
		13:32	73°48.279	128°09.871		CTD	70.7 cm
		13:39	73°48.236	128°10.016		CTD	71 cm
		13:46	73°48.202	128°10.179		CTD	63 cm
		13:53	73°48.178	128°10.358		CTD	80 cm
TI 08 26	4.5.2008	12:30				Start EM-Bird profile	
		15:10				End of EM-Bird profile	